TEMPORAL ENCODING IN THE VISUAL SYSTEM

by

Maier Almagor

Dissertation submitted to the Graduate Faculty of the
Virginia Polytechnic Institute and State University
in partial fulfillment of the requirements for the degree of
DOCTOR OF PHILOSOPHY

in

Industrial Engineering and Operations Research

APPROVED:

Harry M. Snyder, Chairman

M. H. Agee

D. L. Price

A. W. Bennett

A. M. Prestrude

July, 1977

Blacksburg, Virginia

ACKNOWLEDGEMENTS

This research was partially supported by Contract No. F33615-76-R-5022 from the U.S. Air Force Aeromedical Research Laboratory.

The author acknowledges the assistance of all his graduate committee, and especially the encouragement and critical comments of .

Special thanks are extended for for the help provided in the design and construction of the equipment and for valuable comments.

TABLE OF CONTENTS

TABLE OF CONTENTS (Continued)

LIST OF FIGURES

LIST OF FIGURES (Continued)

LIST OF TABLES

INTRODUCTION

An image falling upon the retina of the human eye excites millions of receptors (cones and rods). The visual system has the formidable task of interpreting the image, or temporal and spatial pattern of excitation, to allow the human observer to perceive form, color, depth, and movement.

To fully understand spatial and temporal visual perception, one must relate the physical stimulus to the physiology of the receptors, the manner in which the central nervous system handles the signals received from the receptors, how those signals are encoded, and what kind of signal processing is performed. This is a most complex subject which has generated thousands of research efforts and papers over the last two centuries. It is by no means completely understood, although great progress has been made in quantifying many aspects of visual perception. With such quantification efforts have come several conceptual and mathematical models of both the spatial and temporal processes of the visual system. To date, none of these models has adequately described and predicted either the spatial or the temporal information processing of the system. In part, the failure of existing models is due to a lack of integration of the spatial and temporal dimensions.

The purpose of this dissertation is to develop an integrated conceptual model of encoding the spatio-temporal information by the visual system, and to test this model with several pertinent laboratory experiments.

Temporal Information

The eye transforms the physical energy of the incoming visible radiation into neural activity, which in turn creates the psychological sensation of brightness.

The visual system extracts from the incoming photons information representing both their spatial and temporal distributions. Conceptually, one can think of this process as that of encoding the neuronal activity with different codes and then decoding it in a "central processor". The study of the temporal encoding in the visual system is particularly important to psychophysics because the encoding is indicative of the nature of the signal processing mechanism in the eye-brain system. Temporal encoding is usually studied in flicker-fusion experiments, which, because of their relative simplicity (involving only a single dimension stimulus), flourished in the last several decades. An exhaustive survey of the flicker-fusion research literature can be found in Brown (1965).

Due to the ease of implementation, the square-wave time varying stimulus was historically the most common temporal pattern of stimulation. In more recent years, the sinusoidally varying temporal stimulus has been used frequently. A sinusoidal stimulus can be described by the function

$$L = L_0 \ (1 + m \cos \omega t) \qquad (1)$$

where L_0 = mean adaptive (usually mean stimulus) luminance

L = current value of luminance,

m = modulation coefficient defined by:

$$m = \frac{L_{max} - L_{min}}{L_{max} + L_{min}},$$

ω = temporal frequency = $2 \pi n$,

n = number of cycles per second (Hz), and

t = time in seconds.

It is well known that complex waveforms can be described in terms of sinusoidal components (fundamental and higher-order harmonics). It has often been argued that the visual system acts like a Fourier analyzer, decomposing a complex waveform into its components and processing them as a linear system, that is, summing their individual outputs.

There is some objective evidence (Brown, 1965) that the physiological response follows the fundamental of the stimulus, but does not exactly duplicate the waveform, becoming more and more sinusoidal-like as the frequency of the stimulus increases. With a sinusoidal stimulus, experiments are easier to design and results easier to interpret because one can separate the mean (steady) luminance from the modulation and frequency of the waveform.

Nature of temporal sensitivity. For every level of adaptation luminance and frequency of the stimulus, a temporal modulation can be found at which the flicker is no longer perceived (fusion). The first researcher to carry on a thorough analysis of this kind of

flicker research was De Lange (1954; 1958; 1961). His results are summarized in what is generally called a set of De Lange curves (Figure 1).

De Lange's data show that, at higher adaptation levels, the response of the operator seems to present a resonance or maximum response at a frequency of 4-10 Hz, depending on the adaptation level L_0. Stimuli which barely flicker at the "resonant" frequency are fused below and above this frequency. For frequencies below 2 Hz, the curves asymptote and remain at a constant modulation coefficient. De Lange utilized a 2-degree visual stimulus field, surrounded by a 60-degree fixed luminance border.

Kelly (1959; 1960; 1961a; 1961b; 1961c; 1966; 1969; 1971a; 1971b; 1972; 1975a; 1975b; 1976), who is probably one of the most prolific researchers in the flicker domain, reasoned that a small field surrounded by a steady zone might result in spatio-temporal variations at the borders of the test field; thus, the observer would report a perceived temporal variation though he might have made a spatial judgement.

Kelly used a large, 50-degree, stimulus field, surrounded by a tapered-to-zero 18-degree region, which he calls a "Ganzfeld". Kelly's results (Figure 2) are similar to De Lange's curves in the high frequency region. As predicted, they differ in the low frequency region where they show less sensitivity than do De Lange's data.

In all but the very low level of adaptation, two trends can be observed with increasing frequency: (1) an increase in sensitivity

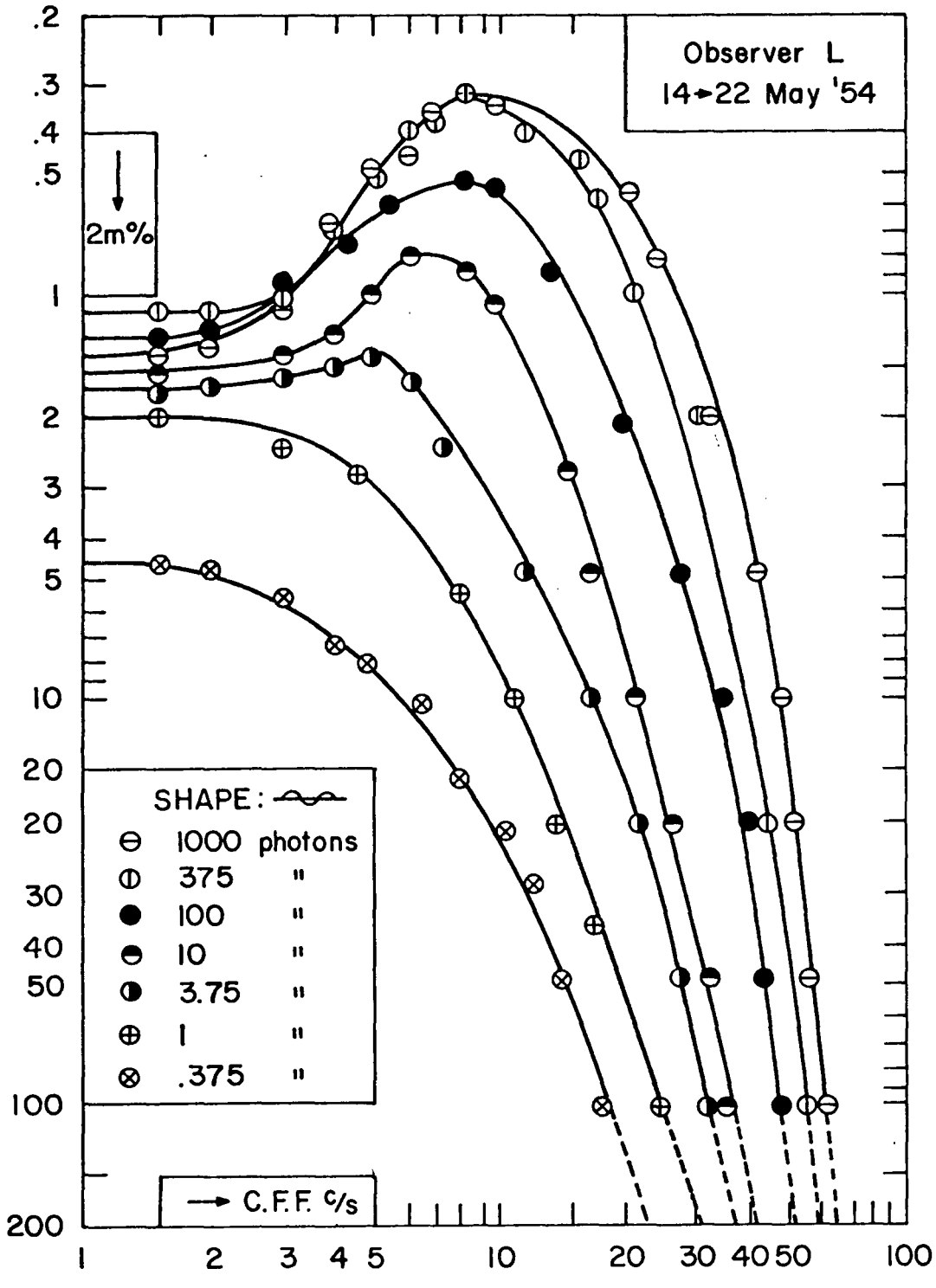

Figure 1. De Lange's (1966) results

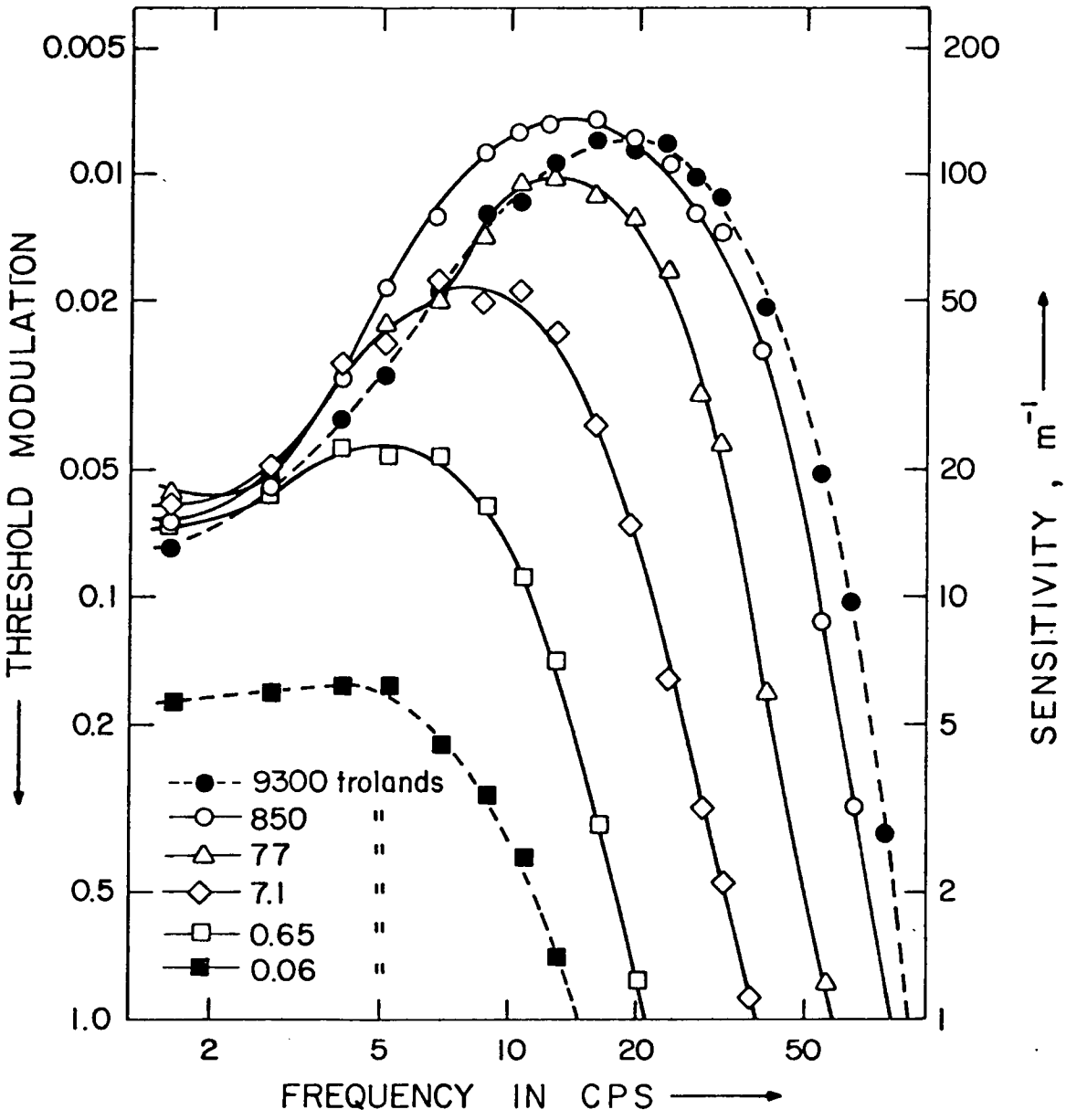

Figure 2. Kelly's (1961) results

up to some maximum value; and (2) a steep decrease to unity modulation after the maximum.

With increasing mean adaptation luminance level, the maxima response points are greater in sensitivity (less in modulation) and shifted towards higher temporal frequencies.

Previous temporal models. Several models have been offered to explain the response of the human operator to sinusoidal varying stimuli. First, De Lange (1961) presented an analog model including 10 RC filters connected in series with two LRC filters (Figure 3). This model, while following closely the experimental results at some brightness levels, does not explain the changes occurring with different adaptation levels. As De Lange points out, the values needed in the analog model (C = 250 μf, L = 1 H) are incompatible with living physiological systems.

Levinson (1968) proposed a model based on a multiple stage integrator with leakage. His model is expressed as

$$\Delta P = \int_0^{\Delta t} [a(\bar{L} + \Delta L) - f(P)]\, dt \qquad (2)$$

where: P = photoproduct concentration,

ΔP = small change in photoproduct concentration,

a = constant,

$\bar{L}$ = mean luminance,

ΔL = departure of L from $\bar{L}$, and

$f(P)$ = photoproduct decay (leakage), proportional to P.

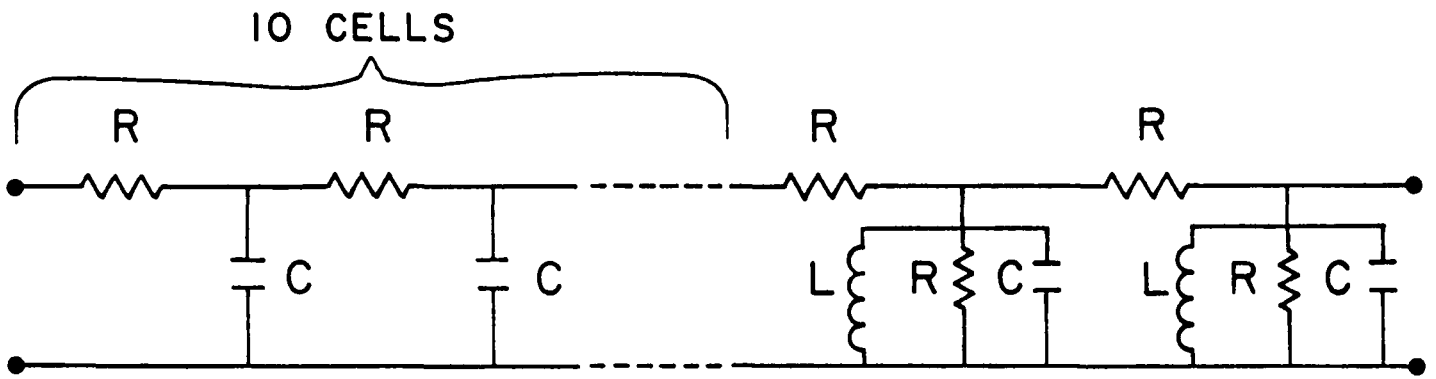

Figure 3. De Lange's electronic analog model

When several similar integrators (up to 10) are connected in cascade, they can be represented by a multiple stage, low-pass filter which can be made to fit the slope of the De Lange curves at high frequencies, but not at the lower end.

Sperling and Sondhi (1968) proposed a model built of four main components. The components of their model are (1) a 2-stage filter whose time constants are controlled by parametric feedback, (2) a feed forward filter whose time constant is controlled by its input, (3) six linear low pass stages, and (4) a threshold detector. This complicated model predicts the high frequency part of the De Lange curves, but fails to match the response at frequencies lower than 10 Hz.

The most elaborate flicker theory is probably the model proposed recently by Kelly (1971a). The model incorporates a linear diffusion process of the photosubstance in the receptors (based on a model derived by Veringa (1970)), which accounts for the high frequency part of the De Lange curves, and a lateral inhibition-summation process in the retina, represented by up to 10 variable-gain, cascaded-feedback integrators, which is responsible for the low frequency part. The original theory of linear diffusion, developed by Veringa (1970), incorporates a term which represents the losses *inherent* in diffusion processes. Kelly equates this term to zero on the grounds that, with losses, the theoretical response does not fit the experimental results.

Thus, to date, no unitary model satisfactorily accounts for all of the flicker-fusion experimental results. In order to predict

these results, a new conceptual model, which follows, has been developed.

Temporal integration. A predictive temporal model of the visual system must account for the several relationships noted above in De Lange's and Kelly's results. Moreover, it must also predict the changes in temporal integration time with changes in the luminance of the adapting stimulus.

It is well known that the eye-brain system integrates visible radiation over time and space, and that this temporal and spatial integration varies with the level of retinal illuminance (Block and Ricco Laws). Herrick (1956) studied the luminance discrimination of the fovea as a function of the duration of the decrement or increment in illuminance. His results, which are pertinent to the development of the proposed model, are summarized in Figure 4. It can be seen that for times shorter than the integration time (called "critical duration" by Herrick), illuminance and time can be interchanged (log $\Delta I \cdot t$ versus log t is constant).

The integration time varies with the mean retinal illuminance as can be seen from Table 1. The results are for one observer, and the units are transformed to trolands by taking into account the artificial pupil of 3 mm diameter utilized in the experiment. For adapting luminance greater than 50 mL, the diameter of the pupil is smaller than 3 mm (De Groot and Gebhard, 1952), so the calculated pupil diameter was used in estimating the retinal illuminance in Table 1.

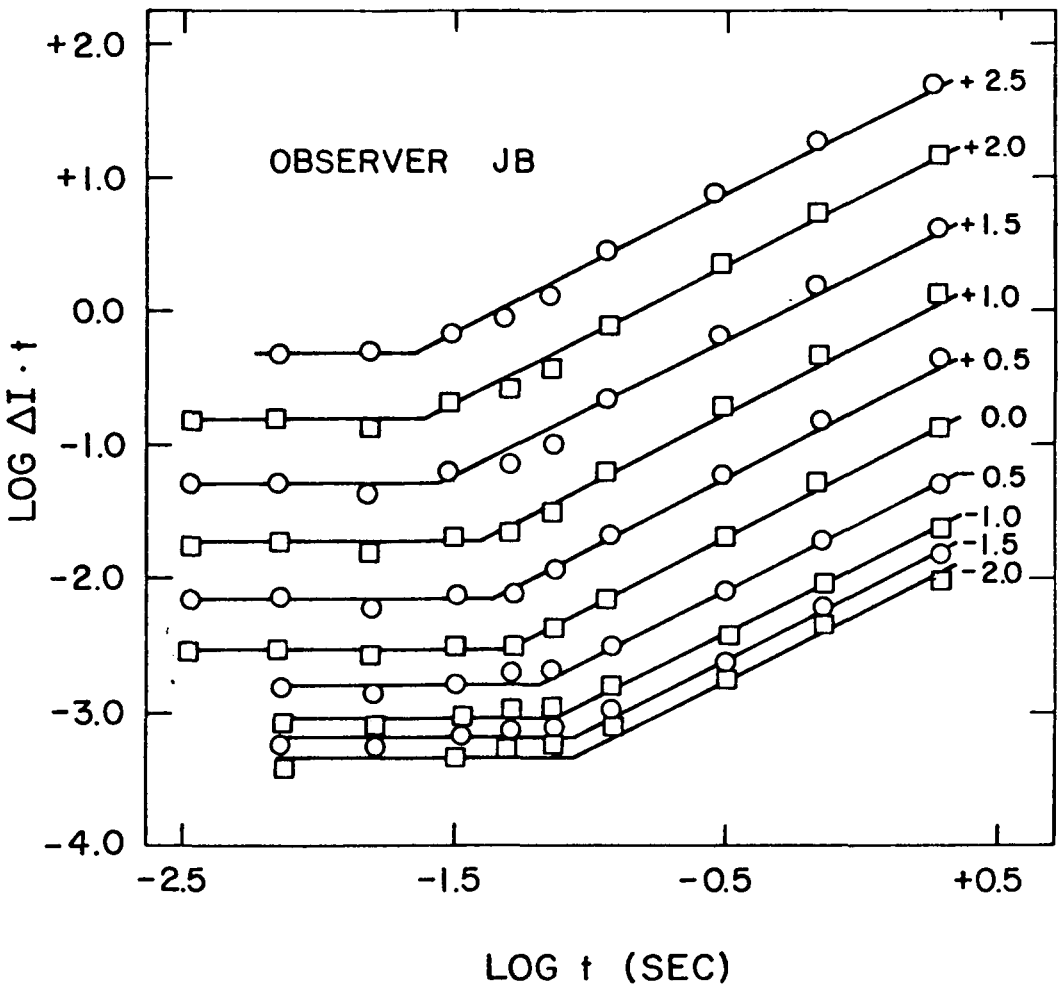

Figure 4. Herrick's (1956) results

Table 1. Herrick's results.

Adapting illuminance, trolands	Critical duration, msec.
4665	21
1930	24
711	27
225	33
71.1	50
22.5	54
7.2	68
2.25	87
0.72	93
0.225	105

Stevens (1966) studied brightness perception as a function of luminance and duration by matching brightness to brightness and numbers to brightness using data collected by Raab. The results show the same trend as Herrick's (Figure 5). The integration times are given in Table 2. The adapting luminance levels, which were originally presented in Lamberts, are translated to trolands by using the mean diameter of the pupil from De Groot and Gebhard (1952).

From Kelly's (1961) results and from Tables 1 and 2, it can be seen that the maxima of the CFF curves for various illuminance levels occur at frequencies exhibiting a wavelength which is approximately double the integration time at the given illuminance level. In Table 3 are presented the comparative results of Herrick, Stevens, and the half-wavelength calculated from Kelly. Taking into consideration the fact that these are results from completely different methods and from different observers, the data appear very consistent.

Another requirement for a temporal model is to indicate how one can detect a brightness variation in time in the absence of spatial modulation (homogeneous field). Somewhere, a detector should exist which performs a comparison between the incoming signal and the one stored from a previous period in time. If the difference is greater than some given threshold, then one sees a temporal brightness fluctuation.

Spatial integration and its relationship to temporal integration. Ricco's Law states that there is a reciprocal relationship between the illuminated retinal area (S) and luminance (L) at the detection

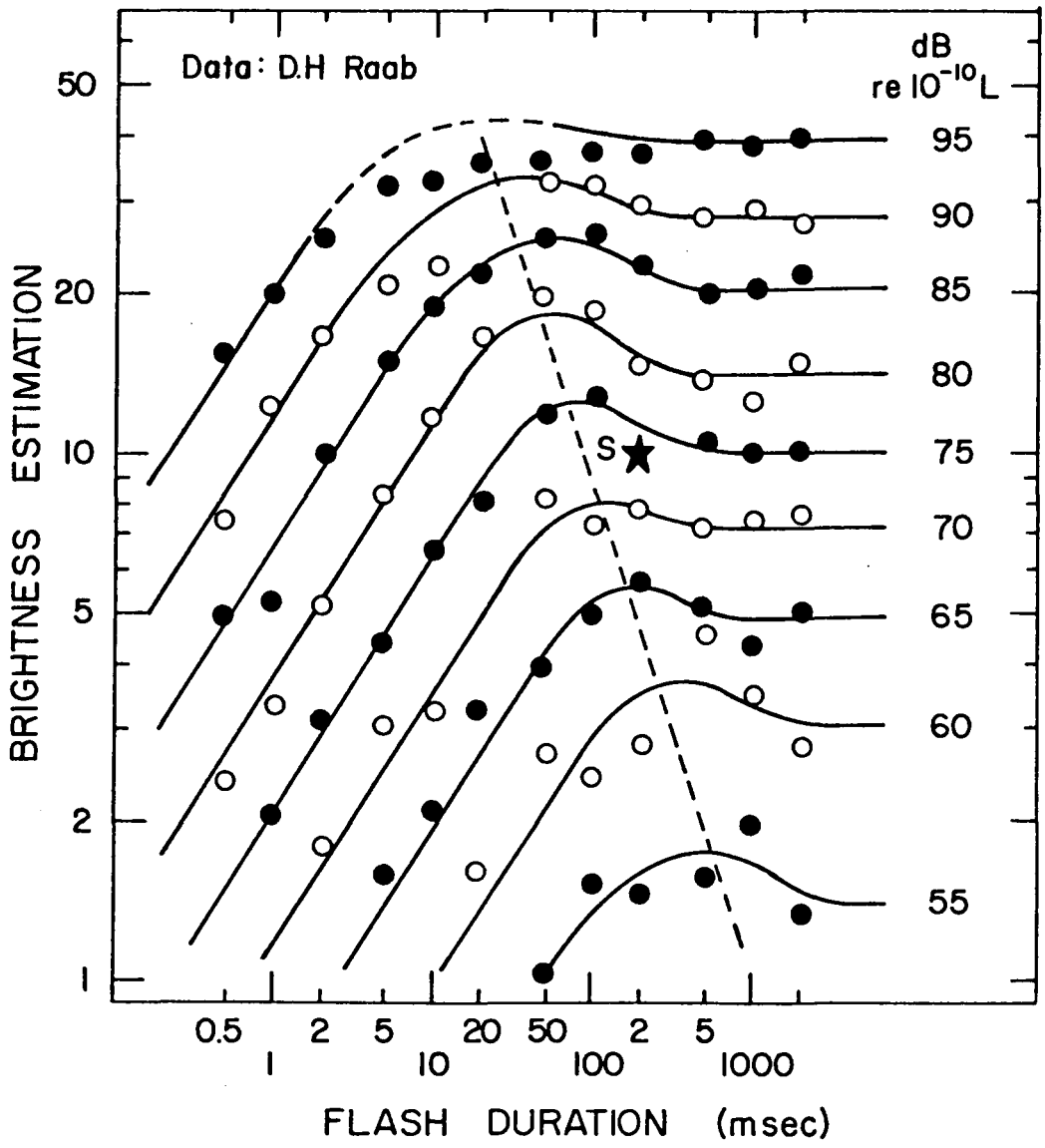

Figure 5. Stevens (1966) results

Table 2. Integration times.

Adapting illuminance, trolands	Integration time, msec.
4460	18
1904	20
846	26
331	32
129	50
48.4	60
17.8	90
6.5	120
2.7	150

Table 3. Integration times and half wavelength.

Illuminance level, trolands	Integration time, (Herrick) msec.	Integration time, (Stevens) msec.	Half-wavelength, (Kelly) msec.
0.7	93	150	110
7.1	68	110	72
77	50	57	46
850	26	26	33
9500	19	17	28

threshold (K), such that $SL = K$. In other words "spatial summation" is a function of luminance just as is temporal summation. At high luminance, there is little or possibly zero spatial summation; at low luminance, large spatial summation reduces acuity.

There is a limit to the applicability of Ricco's Law, however. The diameter of the largest area for which Ricco's Law holds completely in the photopic range is 6-10 arcminutes (Brindley, 1970). Outside this area, a partial summation is achieved (Piper's Law).

There is no available information about the minimum summation area in the central fovea. The one-to-one relationship between the number of cones and the number of optic nerve fibers connected to this area would show a lower limit of zero summation. An acuity of 30 arcminutes obtained under optimal illumination conditions shows the same zero summation (30 minutes of arc corresponds, for a focal length of approximately 17 mm, to 25 μ on the retina, which equals the mean cone diameter (Rodieck, 1973)).

Rather than a fixed spatial summation, the retina exhibits a range of variation for the number of cones involved in the spatial summation. This range is approximately 1:1000 for a variation in illuminance between 0.6 to 600 trolands on the retina (Schlaer, 1937, cited in Graham, 1965).

In the photopic range, the spatial and temporal integration seem to act together as a quantitative adaptation mechanism requiring a minimum energy stimulus to achieve an output signal high enough to pass through the noisy channels toward the brain, and to be successfully decoded there. This relationship appears to be as

follows:

(1) If the energy of the stimulus is high enough, a combination of a short integration time and no spatial summation achieves the best temporal and spatial resolution.

(2) For low energy stimuli, a longer integration time and wider spatial summation can achieve a good signal-to-noise ratio at the expense of spatial and temporal resolution.

(3) Superimposed on this quantitative involuntary relationship, there is a voluntary trade-off between the temporal and spatial summation. When a need for high acuity is present, the spatial summation is reduced, and temporal integration is increased, as demonstrated by the increased temporal summation for the resolution of higher spatial frequency targets (Brown and Black, 1976; Nachmias, 1967; Schober and Hilz, 1965) or by the fact that integration time is longer when a criterion dependent on form discrimination is used than when a brightness criterion is employed (Kahneman and Norman, 1964).

There appear to be no published results which provide the answers to the following key questions about temporal and spatial integration:

(1) How are temporal and spatial integration distributed across the retina? Are they constant or locally controlled and set?

(2) How are they set with respect to the time and space luminance history of the stimulus, and how fast can their value change, i.e., is it a slow or fast adaptation process?

In the development of the proposed model, the following assumptions are made concerning these points:

(1) Time and space integration vary across the retina.

(2) The values of time and space integration can change very fast, *i.e.*, it is a fast adaptation system.

(3) The values of the time and space integration are controlled by one of the neuron layers in the retina (*e.g.*, horizontal cells) and their values are set by the time integral of the stimulus surrounding the specific receptors. The importance of the influence of concentric areas surrounding the receptor decreases exponentially with the radius, as conceptualized in Figure 6.

Assumptions (1) and (2) will be evaluated experimentally in this dissertation, while assumption (3) is based on a model developed by Naka (1972) for the S potential of the horizontal cells. Its validity is enforced by the fact that it can explain the spatial Mach bands, the Hermann grid illumination, and other results.

Temporal Model Description.

A conceptual model is proposed which can describe the whole range of eye-brain performance in the temporal domain. It is composed (Figure 7) of two temporal (I_1 and I_2) and one spatial (Σ) integrators, one controller cell (CONTR), one delay cell (D) with a summing junction (J), and one threshold detector (T). Although Figure 7 contains only three cells for simplification purposes, the actual number of cells interacting with each other is probably

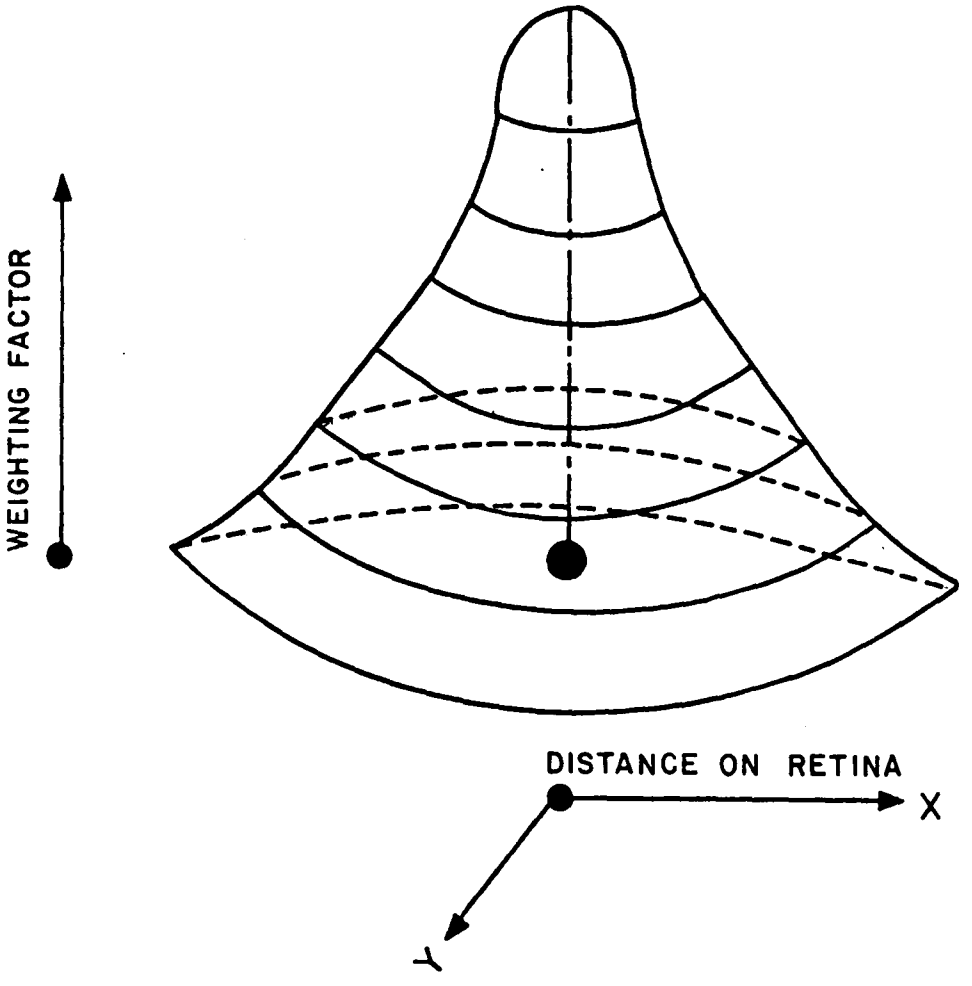

Figure 6. Spatial weighting concept of integration time control

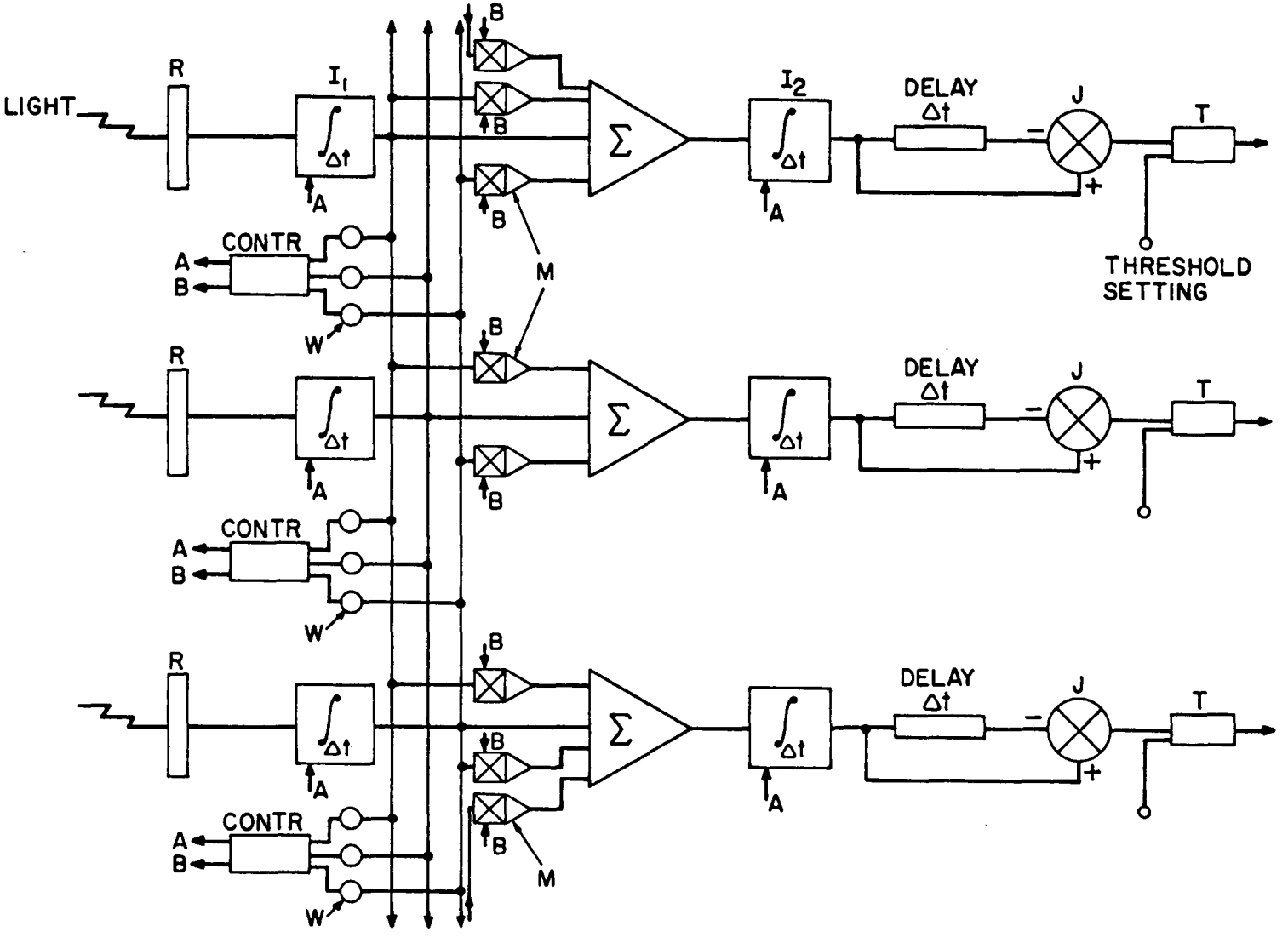

Figure 7. Proposed temporal model

of the order of 1000.

The input light falls upon the receptors R; the transduced receptor output is time integrated in integrators I_1. The integration time Δt is controlled by the controller cell CONTR. The value A of the controlling signal is set by the time and space weighted (through attenuators W) integral of the incoming stinulus. The output from the time integrators I_1 is fed into the spatial integrator Σ. The extent of spatial summation is controlled by the multipliers M through control signal B. The lower the illuminance level on the retina, the higher the control signal B, and therefore the higher the spatial integration extent.

The output of the spatial integrator Σ is once more temporally integrated in integrators I_2 with time integral Δt controlled by CONTR, and imputed to the temporal differentiator which is composed of a temporal delay cell D, and a summing junction J. The output of the summing junction is the difference between the incoming signal and the previous one. If the value of this output is higher than the threshold set for the threshold detector T, a brightness change is perceived.

At the low frequency end, an integrator followed by a differentiator produces an output which increases with frequency. The increase in output continues up to a frequency which has a wavelength (λ) equal to double the time integral (Δt). After the maximum, the output is attenuated due to the integrators (following a $(\sin x/x)^2$ curve) up to a frequency where the wavelength equals the

time integral Δt; at this frequency the output is zero (Figure 8). The output rises again following a $(\sin x/x)^2$ curve for two more smaller maxima at frequencies which are double and triple the frequency of the first maximum before becoming completely attenuated (Figure 9).

If one takes into consideration that there are several million cones and the individual cone time integral is probably normally distributed around a mean value determined by the illuminance level, the superposition of many modulation transfer functions (MTFs) having slightly different integral times will result in the total MTF represented in Figure 9 with a solid line, which looks like the De Lange curves.

Assume that the detection threshold of the temporal detector is independent of the retinal illuminance level. Then, at high illuminance levels, due to a reduction in integration time Δt, the maximum of the curves will shift towards higher absolute sensitivities for the stimuli. The fact that the decrease in integration time is much slower than the increase in luminance level results in a shifting of the maxima toward lower modulation, as in the De Lange curves.

At lower temporal frequencies, the eye requires greater modulation at threshold. As this modulation is increased, however, the spatial summation also increases during the dark halves of the low frequency temporal signal. This increase in spatial summation *increases* the sensitivity of the visual system, thereby reducing the slope of the threshold curve with decreasing temporal frequency.

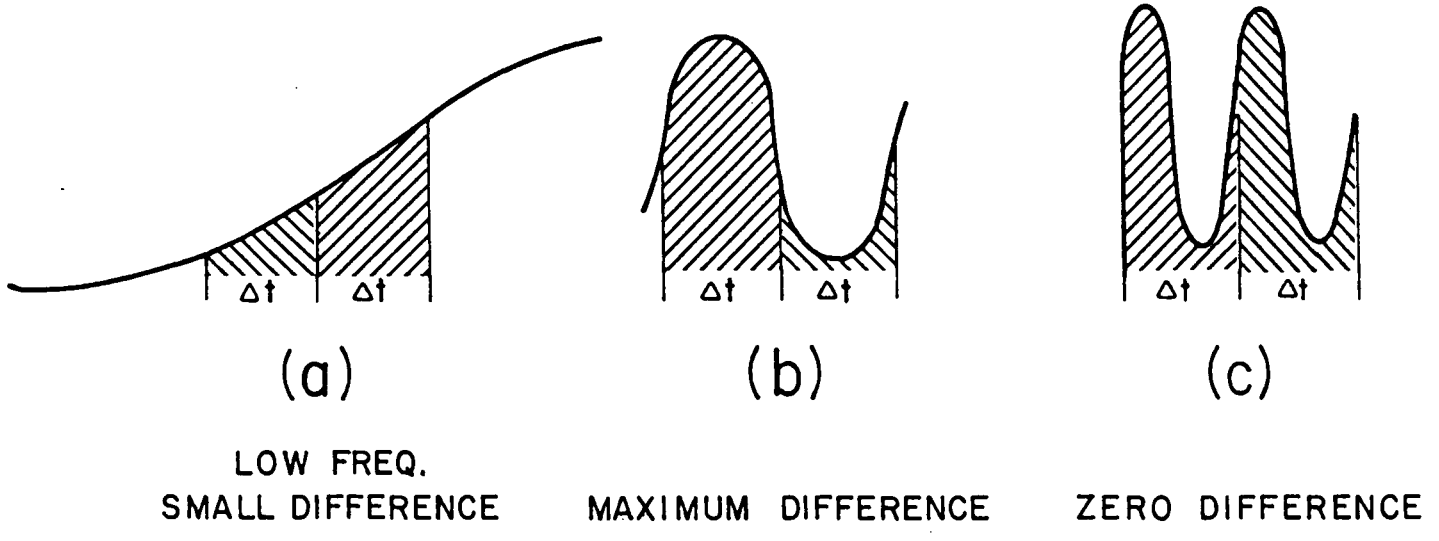

Figure 8. Schematic illustration of temporal model output

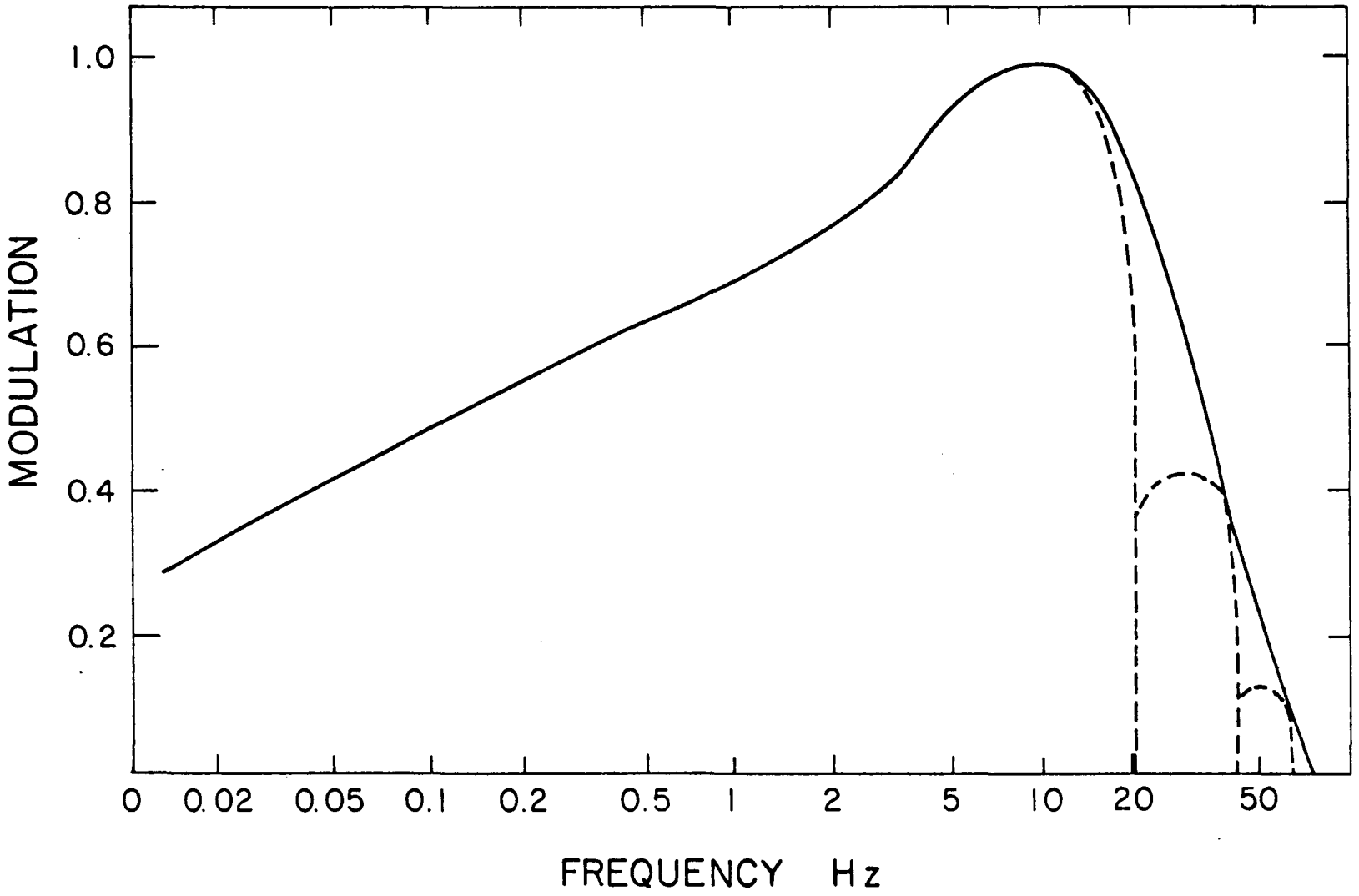

Figure 9. Predicted MTF of the temporal model

As a matter of fact, the proposed model states that the visual system works as a rate-of-change detector in the time domain. If this assumption is true, a small change in luminance dL integrated in a time interval Δt creates the threshold sensation of brightness dB:

$$dL \cdot \Delta t = dB \tag{3}$$

We know that the integration time Δt is inversely proportional to the level of luminance L following some law. Assume that

$$\Delta t = \frac{K}{L} ,$$

where K = constant. Then

$$K \frac{dL}{L} = dB \tag{4}$$

which, when integrated, leads to the well-established logarithmic relationship between brightness and luminance (Fechner's law). Thus, integration time ΔL cannot be constant, and must vary inversely with L.

There exists a misfit between the prediction of this model and previous experimental results of De Lange and Kelly. At very low frequencies, the present model predicts a continuously decreasing sensitivity of the eye; the De Lange curves show that the visual sensitivity remains almost constant at the low end of the frequency scale. One likely explanation for this disagreement is that De Lange's results are contaminated by a spatial rather than temporal discrimination. This fact is more noticeable in the De Lange curves

(4-degree field) than in Kelly's results (50-degree field) but it still exists in Kelly's data.

Yarbus (1967) shows that at rates of change in illuminance lower than some threshold, the eye-brain system does not perceive any brightness variation at all, meaning that there exists some low frequency at which the highest possible modulation will produce rates of change inferior to the threshold, and no change in brightness will be seen. Yarbus' result will be reevaluated in this research.

Direct predictions of the model. If the proposed model is true, the modulation sensitivity of observers characterized by a long integration time will be greater than the sensitivity of observers characterized by a short integration time at the same mean luminance. (For a longer integration time, a smaller amplitude variation is needed in order to be detected.)

Another prediction of the model is that a trapezoidal time varying luminance stimulus will be perceived as having a lower "undershoot" and a higher "overshoot" (Figure 10) which are called "temporal bands". The upper band should be shorter and brighter than the lower band. This is due partially to the hypothesis of integration time controlled by the time integral of the incoming stimulus, and partially to the memory cell working as a differentiator.

At the "upper band" point of Figure 10 the time integral is set by the integral of the incoming stimulus which, at this point, is lower (meaning a longer integration time) than it will be along the subsequent bright constant part of the stimulus, thus creating

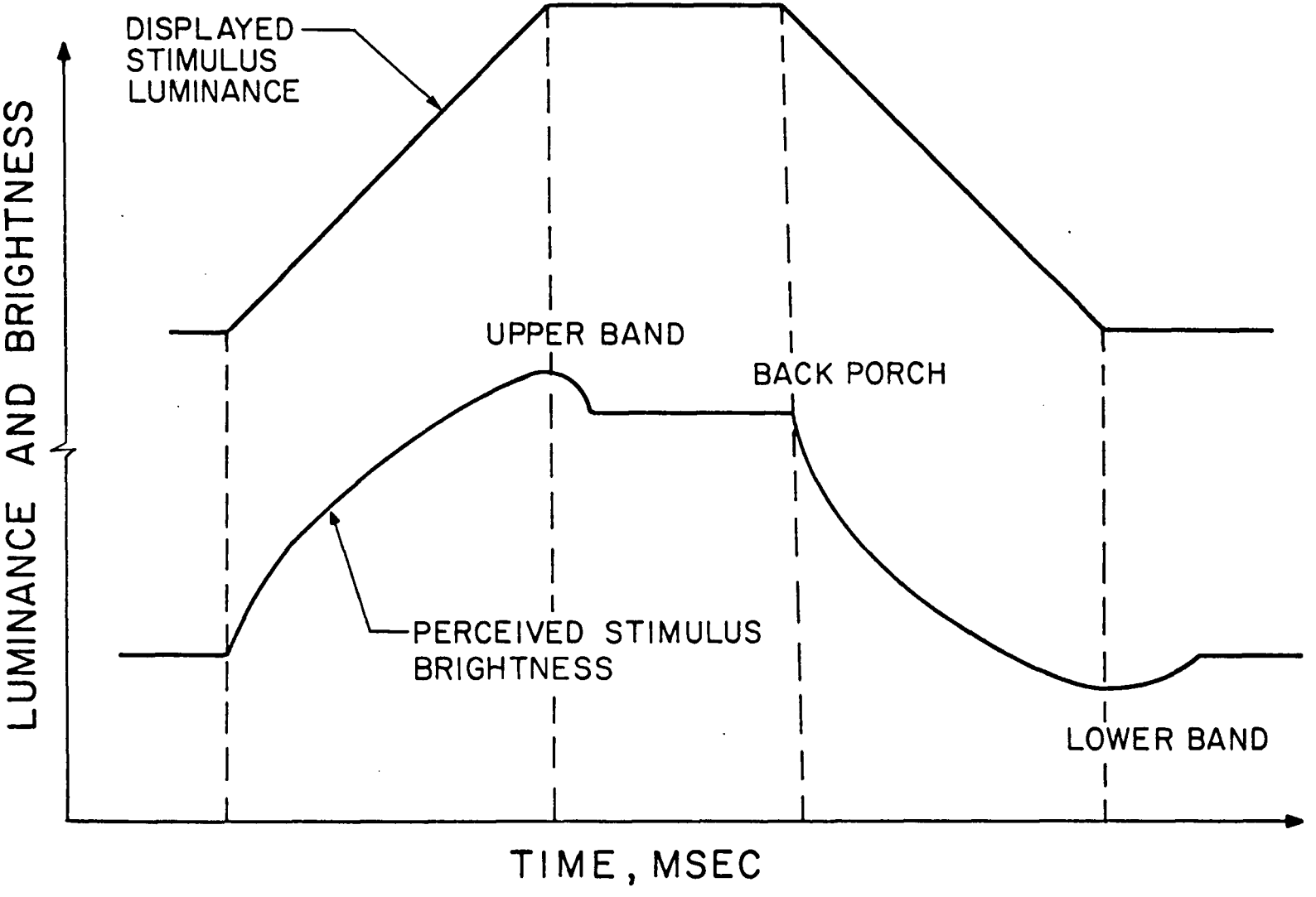

Figure 10. Physical and perceived temporal stimuli

a brighter sensation. Conversely, at the "lower band" point the time integral is set by a higher integrated luminance that it will be subsequently during the dark constant part of the stimulus, resulting in a shorter integration time and creating a darker sensation. The temporal bands are accentuated by the second integrator and by the fact that not only the time integral but also the spatial summation varies in the same way.

One of the weaknesses of the model consists of the fact that it cannot differentiate between different steady state illumination values, *e.g.*, day or night. The information about the mean value of the luminance level might be carried by an alternative channel of information; for example, the value of the integration time itself can be a direct measure of this mean value.

To evaluate the proposed temporal model, the following three experiments were performed, and are described in detail later:

(1) Evaluating the spatial distribution of the integration time across the retina and its dynamics;

(2) Determining the CFF curve, especially the low frequency end, for a very large visual field in which no edges exist; and

(3) Determining the existence of the temporal bands and measuring the factors affecting them.

Spatial Information

The foregoing describes a conceptual model of temporal information processing, the predictions of such a model, and its relationship with spatial summation in the retina. This temporal model is quite over-simplified, however, and requires close integration with a parallel model of spatial information processing.

While the detailed development of a spatial information processing model is beyond the scope of this dissertation, it is necessary and desirable to review the nature of the spatial response of the visual system, to offer a conceptual spatial processing model, and to suggest how the temporal and spatial models are related.

Spatial information processing. Experiments with stabilized images performed by Yarbus (1967) and Keesey (1960; 1972; 1976) show that in a fixated eye, *i.e.*, where the images are stable on the retina, there is no spatial discrimination; the image fades out.

All these experiments show that there is a threshold temporal rate of change of the retinal illuminance under which spatial discrimination cannot exist. In normal vision this rate of change is provided by the eye movements.

The spatial MTF of the eye-brain system (Watanabe, Mori, Nagata and Hiwatashi, 1968; Van Meeteren, 1974) bears a striking qualitative similarity to the temporal MTF. Each individual spatial MTF curve looks like a De Lange curve, and there is the same shift of the maxima toward higher frequencies with increasing illuminance. Accept for a moment that the temporal and spatial curves are similar because they

are the output of the same kind of mechanism or, more explicitly, because both spatial and temporal information are encoded in the same temporal type code.

For simplification purposes, one can consider a single dimension varying spatial stimulus: a sinusoidal grating across the X direction. The retinal distribution is described by

$$dL/dX = \sin X \tag{5}$$

What kind of operator can transform this spatial distribution into a temporal varying signal dL/dt? A spatial differentiator, dX/dt, can provide the needed transformation. This is a velocity which can represent the movement of the eyes across the spatial pattern.

Watanabe, et al. (1968) show that a 3 to 10 ft-L, the most sensitive frequency (the peak of the spatial MTF curve) is at 0.05-0.06 lines/min of arc. At this luminance, which is equivalent to 100 to 350 trolands, Kelly's temporal curve peaks at approximately 14Hz. To transform the peak from 0.055 lines/min of arc to 14Hz, we need a velocity equal to 14/0.055 = 254 min of arc/sec, or 4.2 deg/sec, or 0.073 rad/sec. If we accept further that the movement of the eyes is approximately sinusoidal ($A \sin \omega t$) at a frequency near the natural frequency of the eye (approximately 80 Hz, cf. Childress and Jones, 1967), the amplitude of the movement can be calculated as follows:

The velocity of the sinusoidal movement $X = A \sin \omega t$ is:

$$dX/dt = A\ \omega \cos \omega t \tag{6}$$

Taking the mean value of $\cos \omega t$ as 0.7 (in the quasi linear interval), and equating the velocity to 0.073 rad/sec, we get:

$$A = 0.073/(0.7\omega) = 0.073/(0.7 \quad 2\pi \ 80) = 0.000208 \text{ rad},$$

$$A = 0.72 \text{ min of arc.} \qquad (7)$$

The transforming movement is thus a sinusoid with a frequency of 80 Hz and amplitude of 0.72 min of arc.

Is there some movement of the eye similar to the described sinusoid? The eye movements can be categorized in three groups (Ditchburn 1973): (1) slow drift; (2) occasional sharp movements or saccades; and (3) oscillatory movement showing a small amplitude and high frequency, called tremor.

The drift is too slow, and the saccades are irregularly distributed over time. The only movement which can provide the needed differentiator is the tremor. Y. LeGrand (1960) suggested that the micromovements of the eye (tremor) transform the spatial frequency to temporal information. However, the study of tremor is made very difficult by its small amplitude (43 sec of arc) and high frequency.

Modern methods for the study of eye movements can be divided into two groups: one utilizing mirrors or lenses resting on the eyeball, and the second utilizing images formed by the eye itself (*e.g.*, first and fourth Purkinje images). By adding a lens (mirror) to the eyeball, the moment of inertia of the eye is changed by up to 200% (Ditchburn, 1973, p. 356), changing completely the dynamics of the movement. On the other hand, due to the high accelerations involved (up to 60 rad/sec^2) the added pieces will slip on the eyeball or deform it, making the obtained results questionable.

The second category of measuring instruments, utilizing images formed by the eye itself, is limited by the error band of its detectors to the study of movements larger than 1-2 min of arc (Cornsweet and Crane, 1973). Added complications are the movements of the subject's head, and the differential movement between the eye and the optical gear due to vibrations in the test environment.

Most results show that the tremor has an elongation of 0.5-2.0 min of arc and frequencies varying widely between 30 and 150 Hz. This wide range of frequencies is unlikely; the eye and its muscles form an overdamped mechanical system (Ditchburn, 1973) which is at least of a second order. With a natural frequency of 80 Hz, higher frequencies will require a much greater amplitude input signal because of the high attenuation (greater than 40 dB/decade).

Thus, although sufficiently accurate data do not exist to verify the proposed model, it is quite plausible that eye tremor with a frequency on the order of 80 Hz and an amplitude about 0.7 arc min provides the necessary spatial-to-temporal conversion.

Spatial Model Description

Figure 11 presents a conceptual model of spatial processing. The signals from the receptors R are transmitted to the integrators I_1 through the switches S, which coordinate the sign of the signal with the direction of the eye movement. A decision center DEC decides (based on spatial information from surrounding receptors) whether or not the

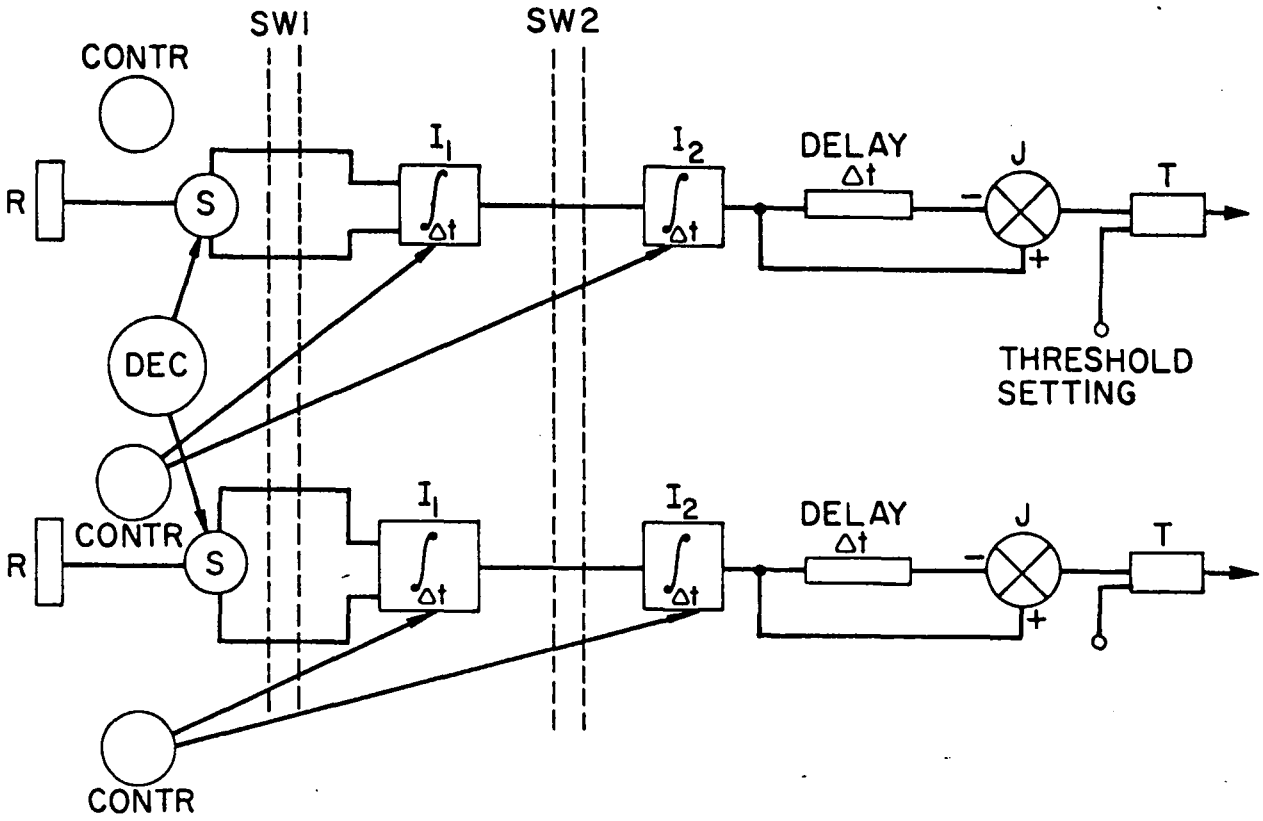

Figure 11. Proposed spatial model

signal is due to spatial modulation (eye movements) or to temporal modulation, and controls accordingly the switches S.

The switching layers SW_1 take care of the correlation between cell signals in case of eye movements other than tremor, switching signals between cells in proportion to the movement, in order to avoid spatial blur.

The signals from different adjacent receptors (within a receptor field) are summed together conformly to some lateral inhibition-summation model implemented in layer SW_2. Then, the composed signal is passed through an integrator I_2 and finally it comes to the temporal delay cell, summing junction J and threshold detector T.

As in the temporal model, the time integral Δt is controlled by the illuminance level on the retina.

According to the model, the threshold of the spatial frequency MTF will rise with increases in frequency due to the steeper spatial slope (differentiated by the eye movements) up to some frequency at which the temporal attenuation net represented by the time integrators will produce the decline at high frequencies.

The combination of these two proposed mechanisms (spatial differentiation and temporal integration) can explain many experimental results.

Evidence consistent with the model. The presented model is a very crude one and the assumptions are too simple, of course, to account for the *entire* gamut of spatio-temporal experimental results. In order to evaluate the possibilities of the model, however, it was applied to

a number of experimental results from previous studies to determine whether there is some basic contradiction between its predictions and the results reported by other researchers.

(1) *Difference between spatial MFT for sine waves versus square waves.*

The model predicts that at low spatial frequencies, the sine wave, due to the eye movement differentiation, will present a much lower sensitivity than the square wave. This difference is attenuated gradually up to the critical frequency, where the time integrators attenuate both sine and square wave alike. Previous experimental results confirm the prediction. Sensitivity to square-wave gratings is greater for spatial frequencies below about 7 c/deg, and approximately equal to sine-wave grating sensitivity at higher frequencies (Campbell and Robson, 1968).

(2) *Spatial versus temporal sensitivity.*

The model predicts that the temporal sensitivity is greater than the spatial; in other words, the threshold for flicker is lower than the threshold for spatial information at the same illuminance, for the integration time (20-200 msec) is 5-10 times longer than the time of one period of the eye movement. To produce the same signal at the final detector, the modulation of the spatial information must be 5-10 times larger than the corresponding temporal modulation.

Yarbus (1967, p. 65) shows that, in a stabilized vision experiment in which the illuminance on the retina is varied linearly in time at various rates (dL/dt), the subject first sees a hardly detectable circle

of light, then at a rate of change $dL/dt/L_0 = 0.3$, he sees some spatial contours. Finally, at a rate equal to 1 he sees the complete spatial information. Unfortunately, there is no information about the rate at which the temporal information is first perceived, but we can safely assume that it is lower than 0.3, meaning that the temporal threshold is at least 5 times more sensitive than the spatial.

Keesey (1972) shows that in stabilized vision the threshold for temporal flicker is 2-5 times lower in modulation than the threshold for seeing spatial information (a line), and varies as a function of temporal frequency; at some 30 Hz both curves are equal, as predicted by our model.

(3) *Perceived spatial MTF varies with stimulus duration.*

This problem was studied by Shober and Hilz (1965), Nachmias (1967), Watanabe, et al., (1968), and Arend (1976a; 1976b).

The shape of the spatial MTF is a strong function of the exposure duration; it exhibits a low frequency improvement for short flash exposures over the level obtained for steady illuminance.

The explanation could be as Arend (1976a) points out, that the onset and offset of the flash produce temporal increments and decrements of retinal illuminance at the peaks and troughs, respectively, of the pattern, with the magnitude of the increments and decrements being determined strictly by the contrast of the pattern. Under those conditions, the decline in sensitivity due to the eye movement differentiation should disappear. This explanation is in complete agreement with the proposed model.

(4) *How many bars make a pattern?*

It is well known that the number of sinusoidal cycles needed for the detection of spatial patterns is constant for high spatial frequencies and increases for low spatial frequencies (Kelly, 1975a).

Savoy and McCann (1975) showed that for spatial frequencies over 15-20 c/deg there is no difference in contrast sensitivity determined with targets of 7.6, 2.7, and 0.83 deg. Below this frequency, the contrast sensitivity increases approximately proportional to the size of the target.

The oscillatory movement of the eyes, with an elongation of 1.46 min of arc, will get a maximum differentiated signal per receptor from a sinusoidal pattern with a frequency of approximately 20 d/deg. For a lower spatial frequency, the signal from the receptors does not contain maximum information; in the summation processes needed to map the original stimulus, the signal-to-noise ratio will be lower, and more cycles will be needed for the detection.

(5) *Perceived spatial frequency varies with stimulus duration.*

Tynam and Sekuler (1974) reported that sinusoidal gratings appear to be of higher spatial frequency when briefly flashed than when presented for longer duration. The effect is restricted to low spatial frequencies (1 c/deg).

The effect may be attributed to an error in decoding the interference between the temporal (on-off of the flash) and spatial information. The on-off of the flash at specific frequencies can be erroneously

decoded as a change in brightness due to eye movements, *i.e.*, spatial information.

(6) *Perceived spatial patterns and colors triggered by temporal modulation.*

If the proposed hypothesis is true that both spatial and temporal modulation are mediated by the same encoding-decoding mechanism, it should be possible that some temporal modulation would be erroneously decoded as spatial by the central processor and vice versa.

Kelly (1966) reported the frequency of visual responses doubled when a sinusoidally modulated spatial stimulus is also sinusoidally modulated in time. Over a certain frequency (spatial and temporal) range, the apparent stimulus spatial frequency is doubled, or apparent motion of the pattern is noticed.

Smythies (1957) and Remole (1973; 1974) reported that the perceived field corresponding to a homogeneous flickering stimulus exhibits spatial patterns (vertical and horizontal bars, herring bones, *etc.*) having no correlation with the stimulus. Above some threshold (in frequency and modulation) the apparent pattern is in oscillatory movement.

In a preliminary experiment, we produced perceived colors triggered by temporal modulation of a spatially flat field. When a green square-wave, temporally modulated stimulus is presented to observers, various colors and forms can be perceived. The perceived colors vary from observer to observer; for the same observer they vary with the frequency and amplitude of the modulated stimulus between yellow, blue, and purple.

The fact that the perceived colors vary with frequency and amplitude suggests that it is not an afterimage effect, but probably erroneously decoded information, as predicted by the model.

(7) *Exposure duration and contrast sensitivity.*

Keesey and Jones (1976) studied the effect of micromovements of the eye and exposure duration on contrast sensitivity. The MTF of the eye for sinusoidal gratings was measured in normal viewing conditions and with a stabilized retinal image for exposure durations ranging from 6 msec to 4 sec. No differences were found between stabilized and nonstabilized image, which led the authors to the conclusion that the important factor in determining the MTF at short flashes is the exposure duration; the movement of retinal image that may take place within the decision time is of secondary importance. They suggested that image motion on the retina, however, has the function of relieving local retinal adaptation.

This conclusion is incompatible with the proposed model. However, a meaningful explanation exists. The apparatus utilized by Keesey and Jones for the stabilization of the image on the retina presents an average stabilization error of 1 min of arc. With a stabilization error as large or larger than the movement to be stabilized, it is impossible to get any effective stabilization at all, and therefore they probably stabilized the slow drift and saccades, but not the tremor. If this is true, their obtained results are well within the prediction of the proposed model. The sensitivity of both "stabilized" and unstabilized images should indeed have increased for increasing exposure

durations up to some 50 msec. For longer exposures, however, the stabilized image should fade out, because of the second integrator and temporal differentiator in the model. The temporal differentiator is receiving the same input from the spatial differentiators (eye movements). Thus, the drift of the spatial pattern on the retina is required for an image *not* to fade out.

Purpose of this research

In this dissertation several tests of the proposed temporal model are made. These are:

(a) Integration time distribution and dynamics are measured using a noise integration procedure.

(b) Flicker sensitivity using a very large field is measured; the frequencies used descend to 0.01 Hz, thereby testing the prediction of the model that sensitivity is not constant in the very low frequency range.

(c) Temporal bands are measured to test the influence of slope and luminance on their width.

The results of these experiments are useful as a validation of the temporal model and as a starting point for future research in this field.

METHOD

Apparatus

Integration time distribution. In the fall of 1975, preliminary experiments were done to understand how the luminance noise is filtered out of a television image by the eye-brain system. During these studies, an interesting phenomena was noted.

When a TV raster-type display containing noise is viewed with the left eye unoccluded and the right eye covered by a neutral density filter, the noise, which looks like uncorrelated "snow" in normal vision, moves in an *ordered* manner: every noise point seems to follow an elliptical-like trajectory. The plane of the ellipse is perpendicular to the frontal plane and parallel to the floor. The points move from right to left "in front" of the display and from left to right "behind" the display.

Changing the neutral density filter to the other eye changed the direction of the movement; increasing the density of the neutral density filter increased the apparent depth of the movement. In short, it looked like a classical Pulfrich stereophenomenon.

This phenomenon is probably caused by a combination of space and time integration which are different for each eye due to the change in retinal illuminance caused by the neutral density filter.

Because of the constraint that noise points appear only along a raster line, the probability that a pair of points will arrive in a time shorter than the integration time (this includes some four frames) at a distance which is smaller than the integration space is dependent on the quantity of noise present. The noise that was used (white noise in a band pass of 20 MHz several hundred millivolts RMS amplitude) produces many such pairs of points. With both eyes unfiltered, and due to the space summation and phi phenomena, the points will look to be in movement in every direction.

Due to the difference in time integration, (caused by the neutral density filter) the same points will be presented to the two eyes with small disparities, creating the sensation of depth as in the Pulfrich phenomenon.

In 1976, Ross published the results of a series of experiments with random points generated by a computer and presented via two separate displays to each eye of an observer. When the points were presented with a time delay to one eye with respect to the other, the elliptical, in-depth motion started. "... The area surrounding the target is perceived as both foreground and background, the foreground moving in one direction and the background moving in the opposite direction.... Foreground and background may combine to give a strong impression of an upright cylinder rotating around its vertical axis." (p. 85)

This result shows that a temporal delay is equivalent to the eye-brain system to a change in integration time caused by a variation

in the mean luminance seen by the eye. This phenomenon can therefore be used as a measuring tool for assessing the spatial distribution of the integration time across the retina, and to obtain some indication of the dynamics of the integration time.

The block diagram of the components used for this experiment is shown in figure 12. The components are:

(1) Conrac QQA 17-inch TV display used at 525 lines per frame;

(2) General Radio Model 1383 random noise generator producing white noise in the frequency band 20 Hz-20MHz between 0.1 mV RMS and 1. V RMS;

(3) TV Sync generator produced by COHU;

(4) A video switch triggered by the sync generator used to switch off the noise during the sync period; and

(5) A video mixer used for mixing the noise with the sync signal to form a composite video signal.

The neutral density filter has a transmission of 2% and is mounted in a mechanical holder.

The mean luminance of the display was set at 15 ft-L, giving the unfiltered eye a retinal illuminance of approximately 500 tr. and the filtered eye approximately 20 tr.

Flicker experiment. As explained in the Introduction Section, it may well be that the field Kelly utilized for his experiments, though much wider than the field utilized by others, is not wide enough to be considered a full spatial-modulation-free experimental tool. In this

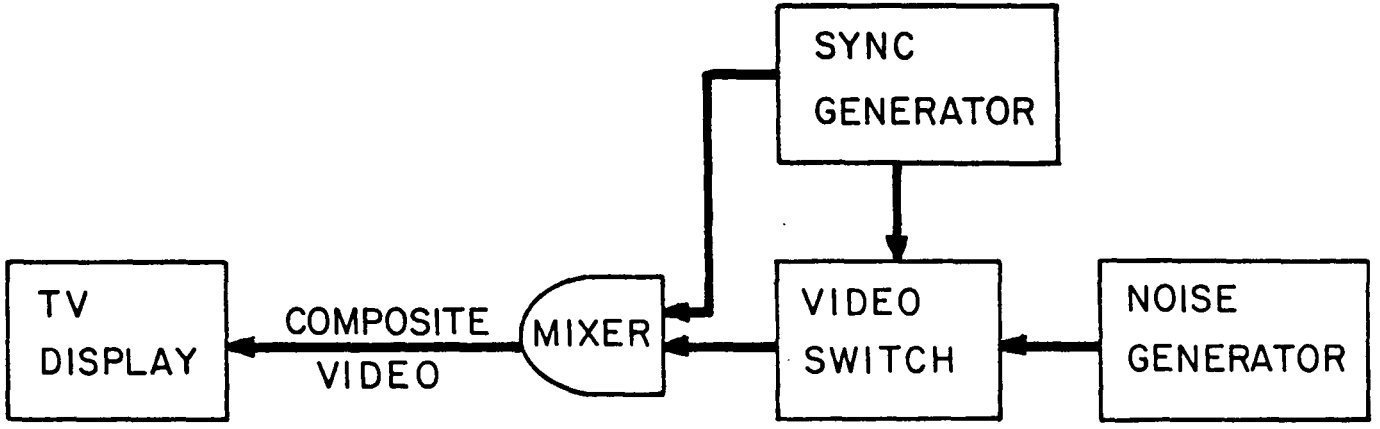

Figure 12. Bloc diagram of equipment for integration time distribution experiments

research, a much larger field (approximately 150 deg) was used; this field can be considered a Ganzfeld (complete field).

The large field used introduces a new variable. In effect it is known that the critical flicker frequency varies widely with changes in the retinal locus of stimulation (Brown, 1965, p. 225; Le Grand and Geblewicz, 1938). This fact, which is probably due to the different integration times of the several types of receptors existing in the retina, probably also contaminated Kelly's (50^{o} field) results.

In order to separate the peripheral cones from the central ones without imposing any spatial borders, one can utilize a spectral separation. In fact, it was shown by Weale (1953) and cited by Le Grand (1960, p. 108) that the spectral sensitivity of the 45 deg cones is much lower than the sensitivity of the foveal cones in the range of 0.55 to 0.7 microns. The field was therefore covered by a #815 orange filter produced by Edmund Scientific having a transmission curve shown in Figure 13.

The light source is an electroluminescent panel produced by Grimes Manufacturing Co. The electroluminescent lamp consists of a layer of phosphor sandwiched between two electrodes, one of which is translucent to allow for the transmission of the usable light, and encapsulated in plastic translucent material.

The lamp uses AC current at frequencies between 60 Hz and 900 Hz, at voltages varying between 50 V and 300 V. The luminance output is approximately proportional to the frequency and to the voltage. At 400 Hz, the lamp has a mean luminance value, and 800 peaks/sec above it (Figure 14).

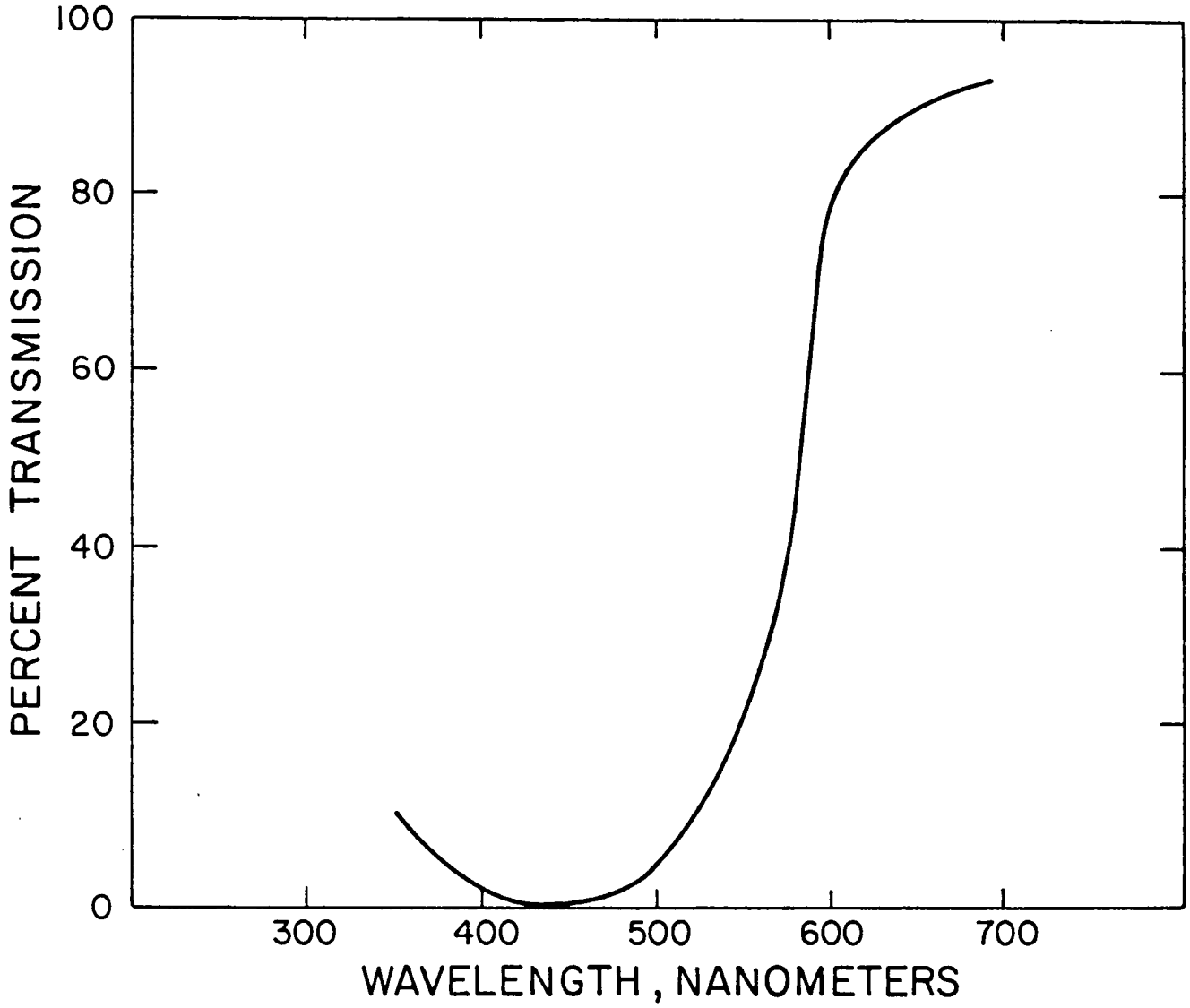

Figure 13. Transmission curve. Edmund No. 815 filter

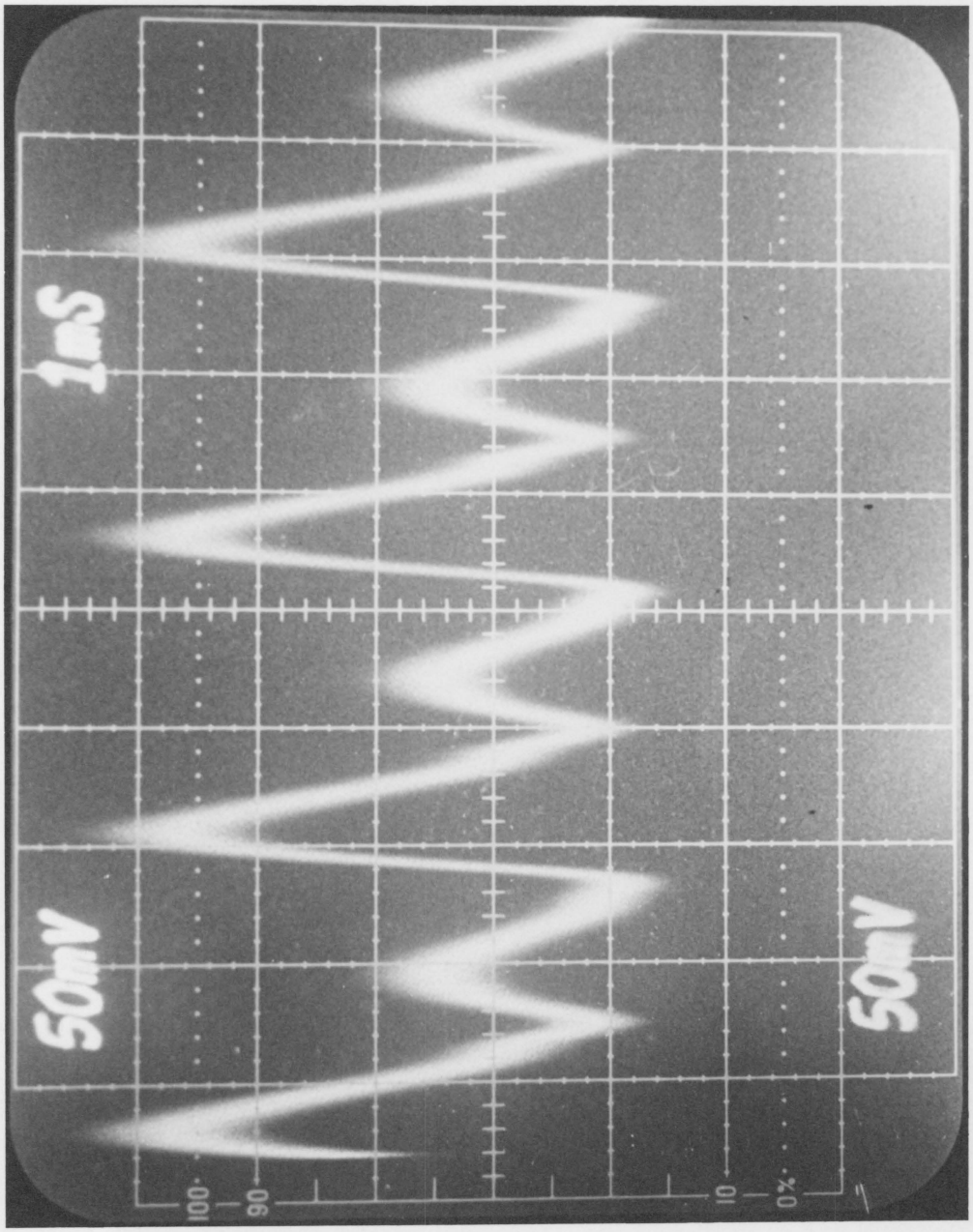

Figure 14. Temporal luminance of electroluminiscent lamp.

Due to the fact that at 800 Hz the eye-brain system integrates the peaks completely, the electroluminescent panel can be considered as a DC lamp. The major advantages of the electroluminescent lamp over other sources are:

(1) It has uniform brightness over the entire area;
(2) It is very fast - less than 1 msec rise and decay time at 400 Hz;
(3) The lamp can be easily shaped to take any form or to fit any configuration;
(4) The spectral composition does not change as a function of brightness;
(5) It can provide a very large surface source (up to 12 in. x 18 in.); and
(6) Its output is easily and linearly modulated by the electrical input.

There are two disadvantages:

(1) It has low to medium luminance output (max 25 ft-L); and
(2) It has limited life time (our experience shows a longer than expected life).

The block diagram of the system can be seen in Figure 15. The components are:

(1) A 940919-W electroluminescent panel 12 in. x 18 in. working at 400 Hz, 240 V.

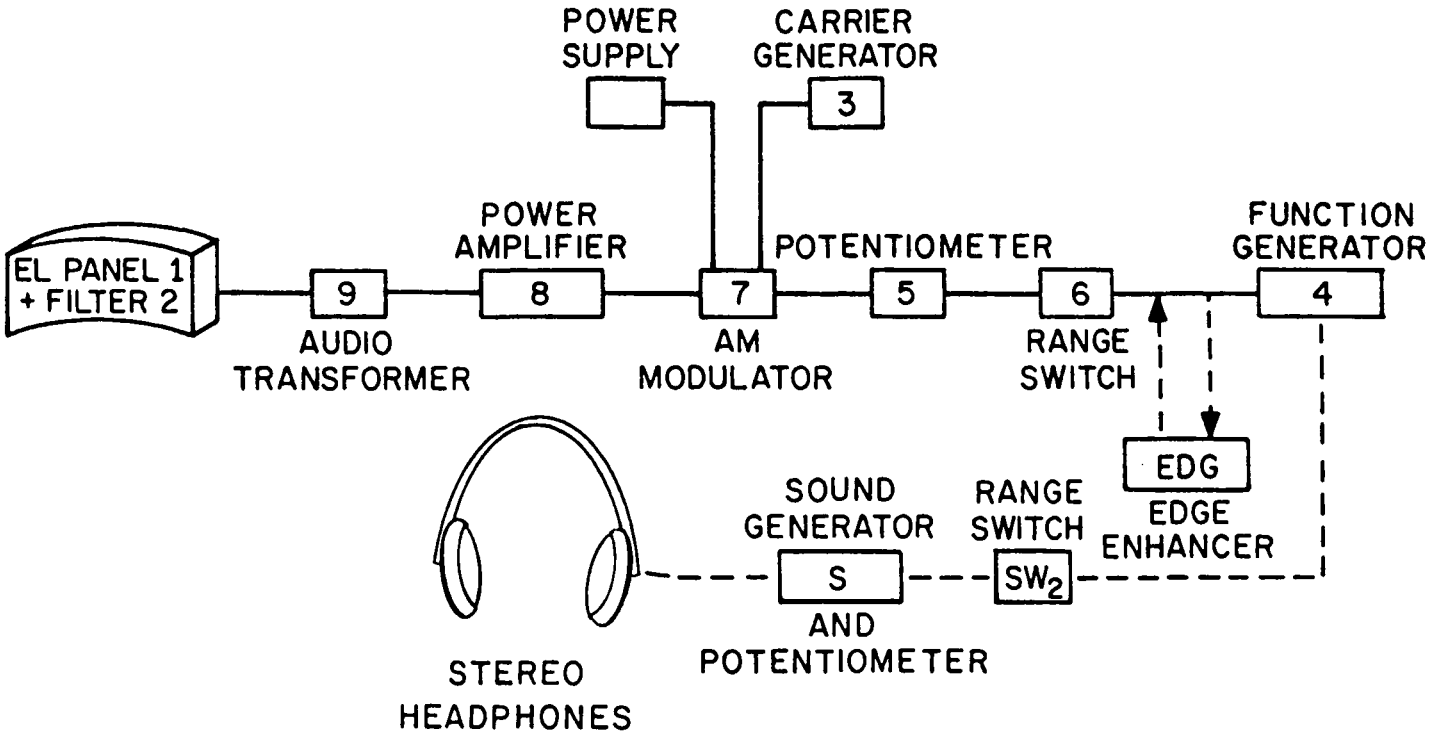

Figure 15. Block diagram of equipment for flicker and temporal bands experiments

Although the panel has a width of 12 in., an electrode runs across the lamp in the middle, leaving an homogeneous surface of 6 in. x 18 in.

The panel is mounted in a mechanical structure having a cylindrical form with a diameter of 14 in., providing a complete field of view for an observer having his eyes near the panel and centered at 3 in. from the top.

(2) In front of the panel and in contact with it is mounted a sheet of #815 Edmund Scientific filter.

(3) A Hewlett Packard #3310 A carrier generator, which generates a 400 Hz sinusoidal waveform.

(4) A Wavetek 164 function generator which generates the modulating function (sinusoidal square, triangular, trapezoidal, etc.)

(5) A 10 turn potentiometer to continuously control the modulation amplitude.

(6) A 10:1 range change switch.

(7) An AM modulator.

The use of the AM modulation was preferred instead of the much easier to implement FM modulation because the output shows nonlinearity as a function of frequency. For a 400 Hz carrier, the side bands are not visible up to a frequency of 80 Hz.

(8) An ALTEC 800-W audio amplifier.

(9) A Peerless 15464 audio transformer.

(10) A digital voltmeter.

(11) A dual trace oscilloscope with memory.

(12) A Gamma photometer used for calibrations.

The 400 Hz carrier is AM modulated by the function generated in the function generator; the output of the modulator is amplified by the power amplifier and raised to the needed voltage by the audio transformer before being applied to the electroluminescent lamp.

The controlled parameters of the modulated wave are:

(1) The form of the modulating wave (square, sinusoidal, triangular, trapezoidal) from the Wavetek function generator.

(2) The frequency of the modulated signal which is continuous between 0.0005 Hz and 100 Hz.

(3) The mean luminance continuous from the power amplifier, measured indirectly by the digital voltmeter.

(4) Modulation amplitude between 0 and approximately 90%, from the 10 turn potentiometer and range switch.

A calibration of the system was performed to check the linearity of the electroluminescent panel and its homogeneity. The microscope of the Gamma photometer was calibrated against a 100 ft-L standard source; then the luminance of the panel as a function of input voltage was measured (Figures 16 and 17).

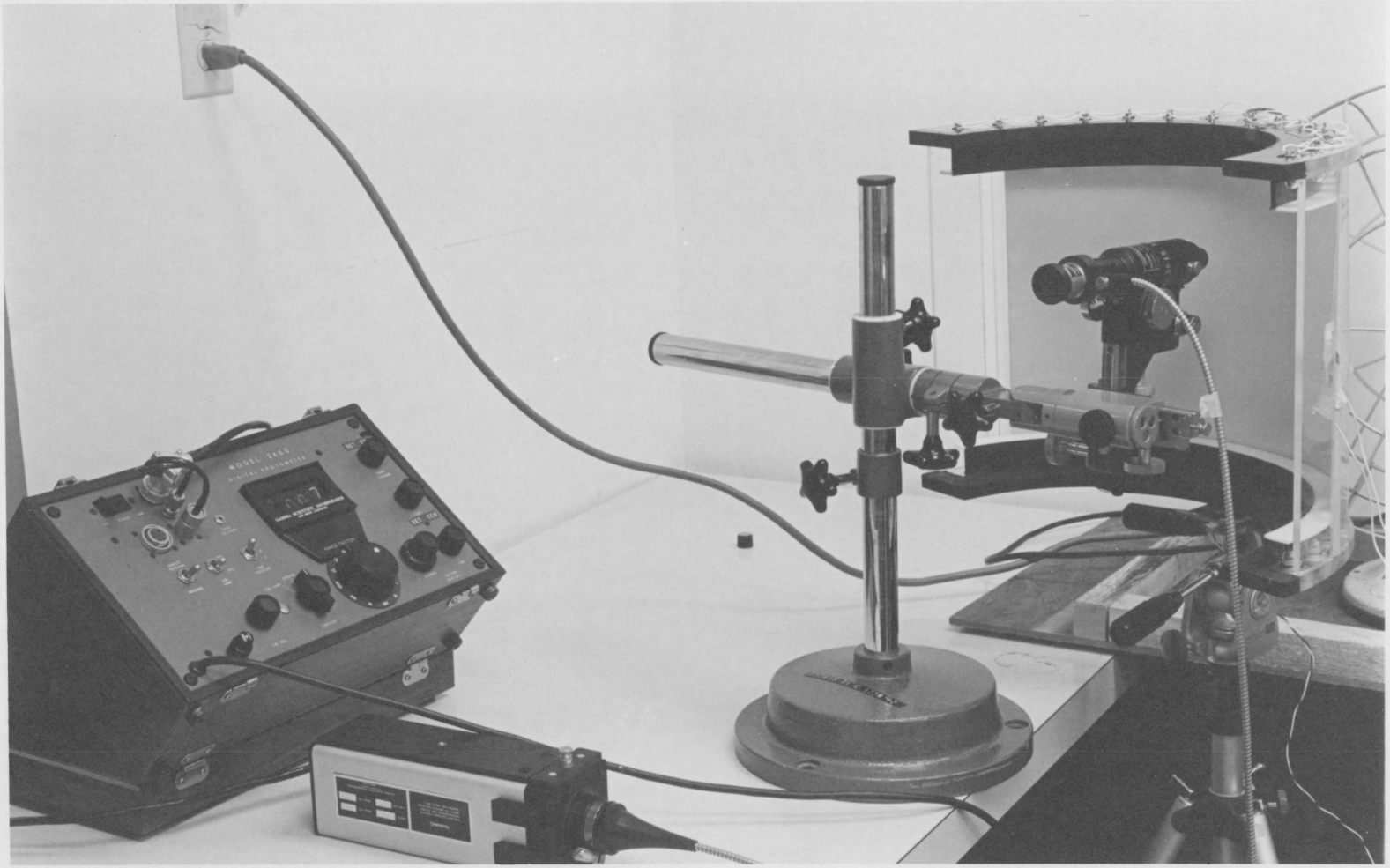

Figure 16. Photograph of equipment calibration setup.

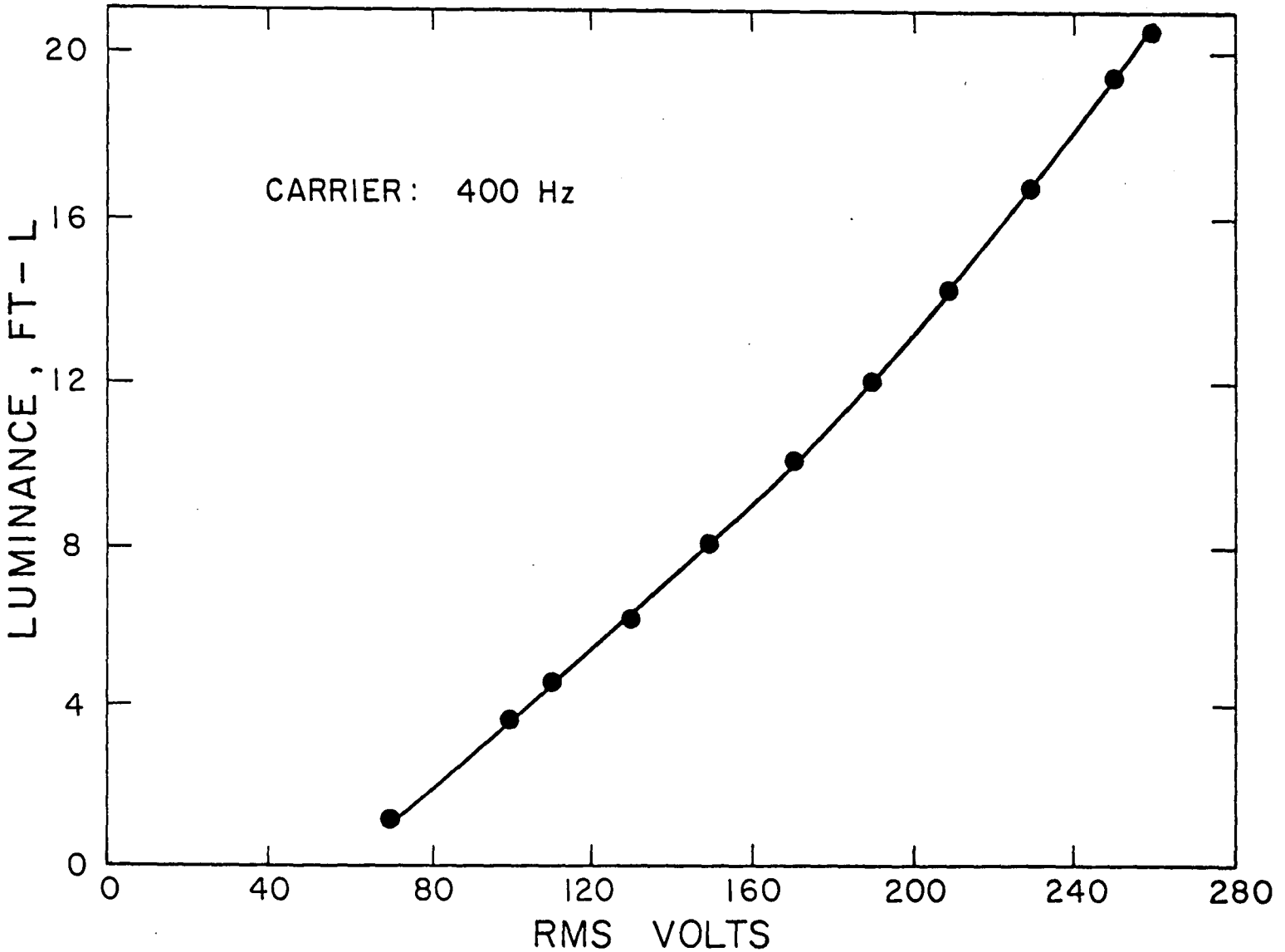

Figure 17. Luminance calibration curve of electroluminiscent lamp

At 150 V, luminance readings at various points of the electroluminescent lamp surface were performed and the difference was found to be less than 3%.

Although some bending of the slope can be seen between the lowest and the highest voltage, one can consider the curve as linear in two parts. Thus, the whole luminance range is usable by taking this fact into consideration.

The electrical waveform was compared against the luminance waveform; no visible distortions were seen (Figure 18).

The system can produce any type of visual stimulus longer than 1 msec for different uses in visual psychophysical experiments. It can produce any waveform that can be imagined with any duty cycle or repetition rate. The usual waveforms are built-in into the Wavetek function generator. Special waveforms can be produced using an analog computer instead of the function generator or by recording them on magnetic tape and replaying them into the modulator.

Temporal bands experiment. To measure the length of the temporal bands a cross-sensory experiment was conducted in which the observer had to control the timing of an auditory stimulus to the point where it appears simultaneously with the *end* of the temporal (visual) bands.

The same apparatus described for the flicker experiment was used. To it were added the following components, indicated by dashed lines (Figure 15).

(1) An edge enhancer EDG. The corners of the trapezoidal waveform produced by the Wavetek function generator are slightly rounded,

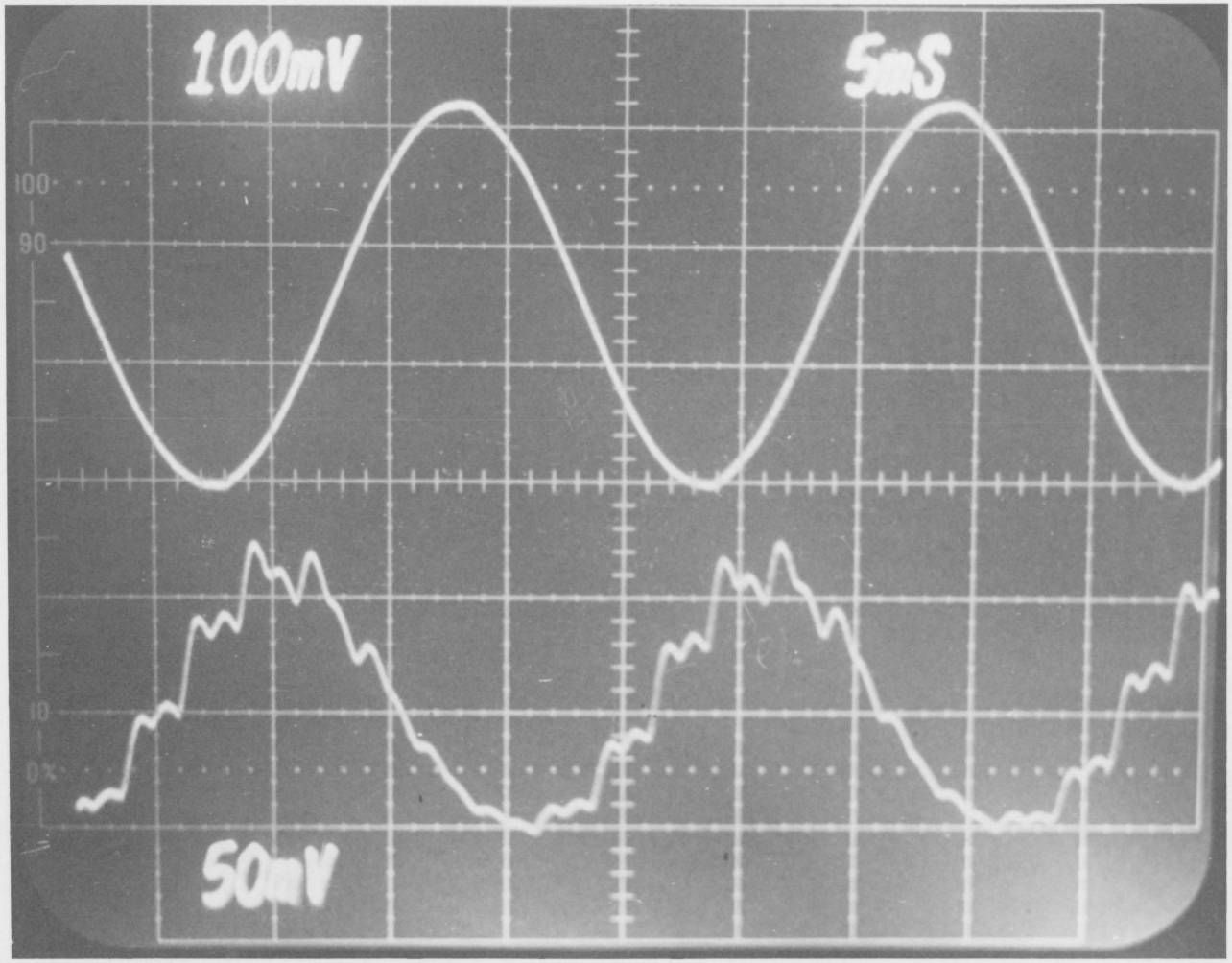

Figure 18. Electrical input and luminance output of electroluminiscent lamp.

which in fact produced less visible temporal bands. A special amplifier was built to sharpen the corners without modifying the other characteristics of the waveform. The resulting waveform was a nearly perfect trapezoid.

(2) A generator (S) of short bursts (3 msec) of 1000 Hz sinusoidal wave, whose output is fed into a pair of headphones to produce the auditory stimulus in the form of a very short tone. The generator is triggered by the trapezoidal waveform and has a range switch (SW2) which selects the leading or trailing edge as triggers and a timer (t) controlled by a potentiometer to position the occurrence of the sound with respect to the triggering point.

By manual control of the potentiometer, the subject is able to temporally position the sound heard in his headphones relative to the luminance waveform on the electroluminescent panel.

The electric signal from the tone generator is also fed into one of the two channels of the oscilloscope.

The controlled parameters are:

(1) Frequency of presentation of the trapezoidal waveform from the function generator;

(2) Modulation amplitude of the trapezoidal waveform from the modulation potentiometer CONTR and measured by the digital voltmeter;

(3) Mean level of luminance from the power amplifier, measured by the digital voltmeter;

(4) Slope of the trapezoidal waveform from the function generator; and

(5) Timing of the auditory stimulus from the tone generator; measured with the oscilloscope. An example of the tone superimposed on the trapezoidal waveform is shown in Figure 19.

Procedures

Integration time distribution. The display was set at 15 ft-L mean luminance, the noise at 250 mV RMS, and a 1.5 neutral density filter was placed in the filter holder.

Ten subjects, all males between the ages of 20 and 50, were asked to sit in front of the display and report verbally their findings about the noise in three experimental situations. The three situations were:

(1) Right eye unoccluded, and left eye covered by the neutral density filter.

The subjects had to report how they perceived the noise; all but one subject saw the noise turning in three-dimensional space.

After seeing the "turning" noise, they had to change the neutral density filter to the right eye and report any changes about the direction of the movement.

(2) Right eye unoccluded and the neutral density filter placed so as to cover only the upper part of the display (as seen by the left eye); at the beginning of the experiment, the

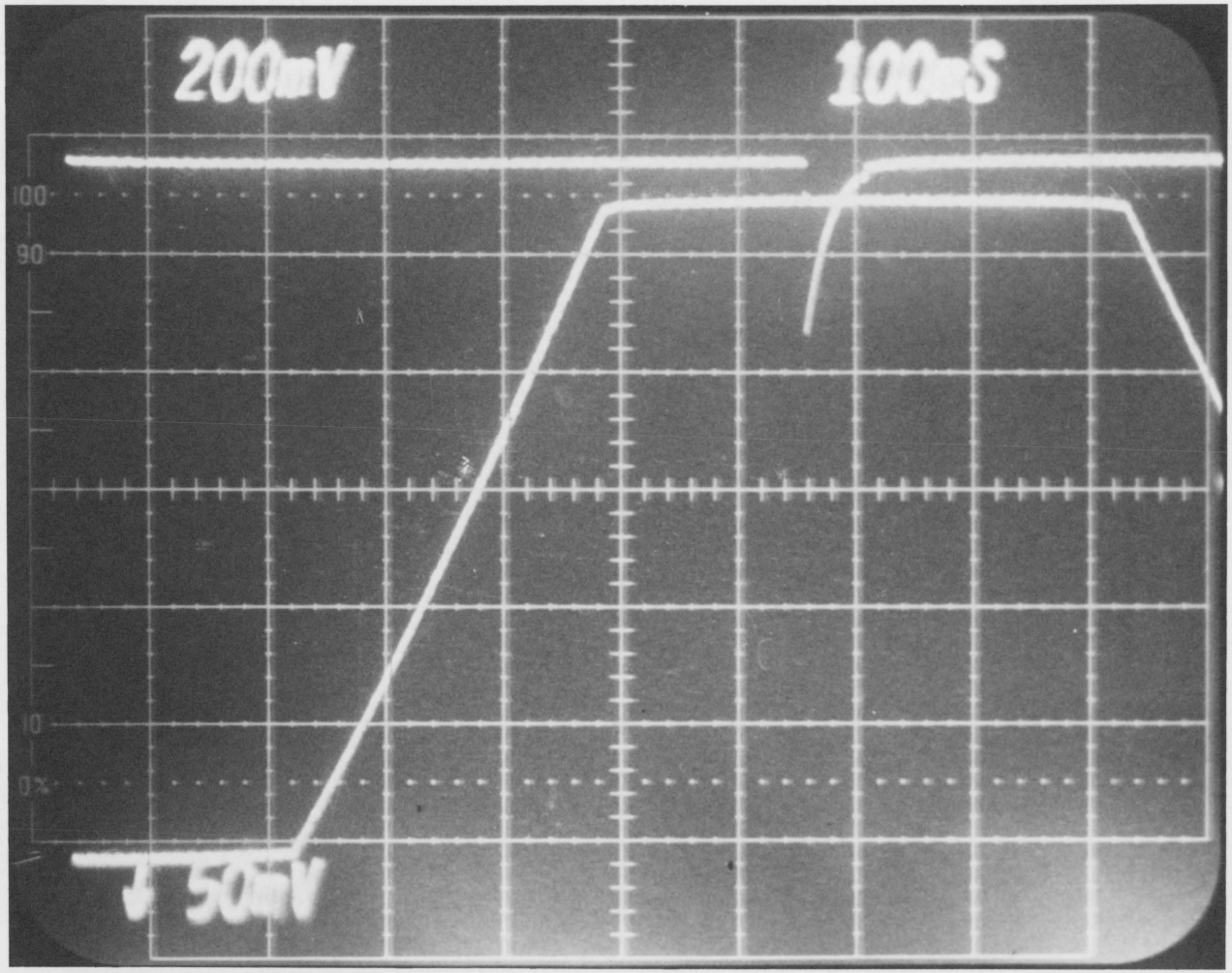

Figure 19. Temporal band measurement displayed on the oscilloscope.

subjects were asked to fixate the lower part of the display and report how they perceive the noise.

After several seconds, they were asked to move suddenly their fixation point to the upper half of the display (covered with the neutral density filter for the left eye) and to describe how fast they perceived the change from "snow" noise to "turning" noise.

(3) The subjects were asked to place the neutral density filter in such a position as to see with each eye half of the display through the neutral density filter and the other half without the filter. The fixation point was at the center of the display (Figure 20). They were asked to report how they perceived the noise.

Flicker experiments. As pointed out above, a very wide field was used for the flicker experiments. To avoid the influence of the pupillary reflex, an artificial pupil is generally used; due to the wide field, this approach is infeasible in the present experiments. Thus, it was decided to paralyze the pupillary reflex with drugs.

The subjects reported to an opthalmologist who, after a complete examination of the subjects' eyes, administered a paralyzing chemical, (1 drop Mydnacyl 1% followed by 1 drop Neosynephrine). The pupils were completely dilated after 10-15 min, and remained dilated for more than four hours. After performing the experiments an antidote was administered (one drop P.V. Carpine) to permit pupil constriction.

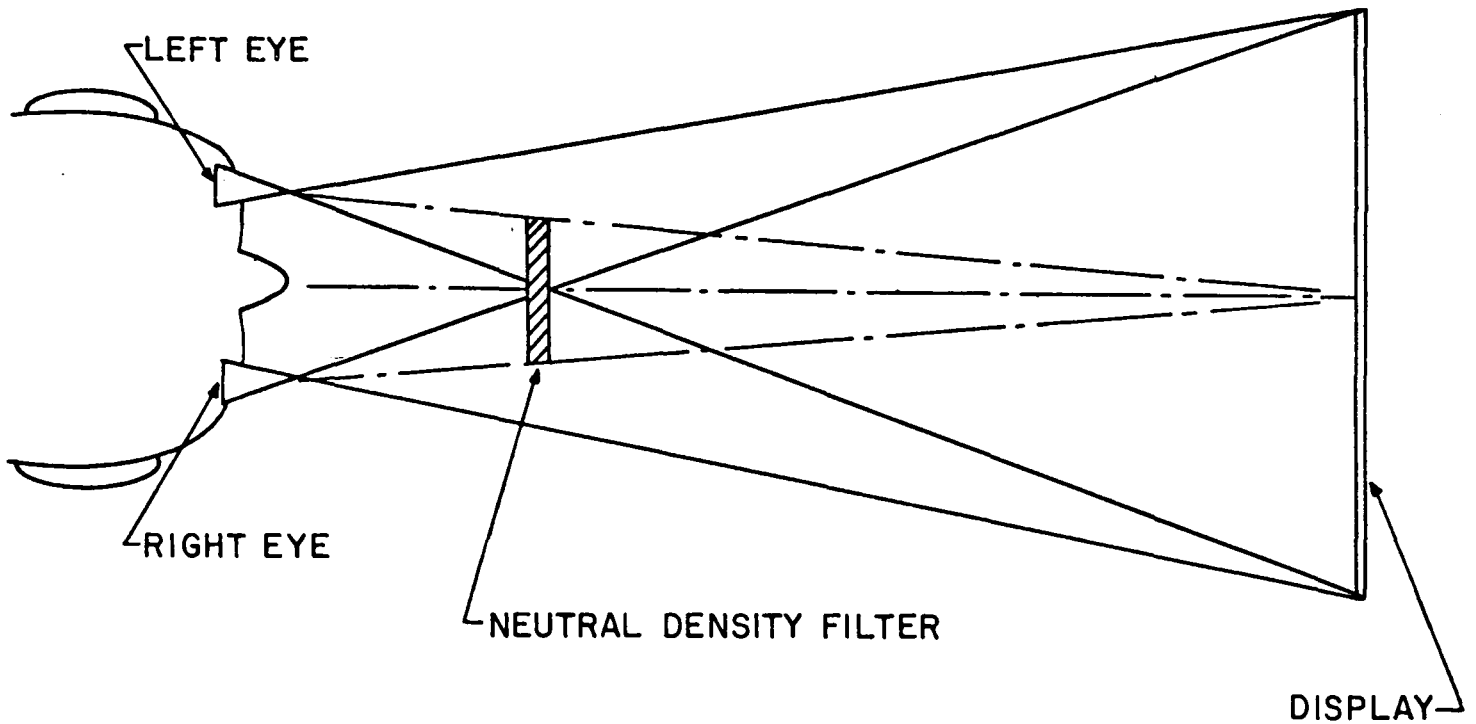

Figure 20. Filtering of eyes for rotating noise experiments

The fact that the paralysis of the pupils lasted only a limited time affected the choice of the numbers of luminance levels, frequencies, and trials.

Two levels of mean luminance, 77 tr and 680 tr, were selected to allow direct comparisons with Kelly's results and yet remain in the linear part of the luminance curve of the electroluminescent lamp.

To set those values, a pupil diameter of 7.17 mm (de Groot and Gebhard, 1952) was assumed. The luminance of the electroluminescent lamp, as measured with the Gamma photometer through the #815 orange filter, was accordingly set at 0.56 ft-L and 4.92 ft-L, respectively.

The selected temporal frequencies cover four decades between 0.01 Hz and 100 Hz. The lowest frequency was 0.01 Hz because the time to complete one trial would have increased too much for lower frequencies. (One trial at 0.001 Hz would have taken probably 2-3 hours.)

The selected frequencies, listed in Table 4, are more densely packed in the region where the CFF curve shows generally the fastest change in slope.

Because of the pupil dilation time constraint, four trials per frequency and luminance level were used. For the 0.01 Hz only two trials were used. The total number of trials was 132, which required the entire four hours.

For each frequency, the subject had two trials starting from zero modulation and increasing slowly to the point where flicker was perceived, and two trials starting from a high modulation where the flicker was easily perceived and reducing to the point where the flicker was lost. The mean result of one pair was considered one trial.

Table 4. Temporal frequencies used in flicker experiment (Hz).

0.01
0.05
0.1
0.5
1
2
4
6
8
10
15
20
30
40
50
60
70

The presentation of the different frequencies was completely randomized (using a random number generator), as was the presentation direction of modulation of each pair (increase *vs.* decrease).

Before starting the session, the subjects had a 5-min adaptation time at the mean illuminance level. The first two trials were discarded as practice trials.

The experimenter set the conditions for the trial (frequency) and asked the subject to increase (or decrease) the modulation to the point where he saw (or did not see) the flicker. The subject then verbally indicated this point to the experimenter who froze the waveform modulation on the memory oscilloscope, measured the modulation, and set the conditions for the next trial.

Every 30-45 min a break of 5 min was imposed.

After all trials at one luminance level were performed, the luminance level was changed and the experiment was resumed after a 5-min adaptation time.

Temporal bands experiment. The purpose of this experiment is to measure the length of the temporal bands.

The expected perceived phenomenon is shown in Figure 21.

To measure the length of temporal bands, *i.e.*, the time between the physical edge of the stimulus and the end of the perceived temporal band, a cross-sensory matching technique was used.

The subject was presented with a succession of trapezoidal waveforms and simultaneously with an auditory stimulus. He could control the phase of the auditory stimulus with respect to the temporal band

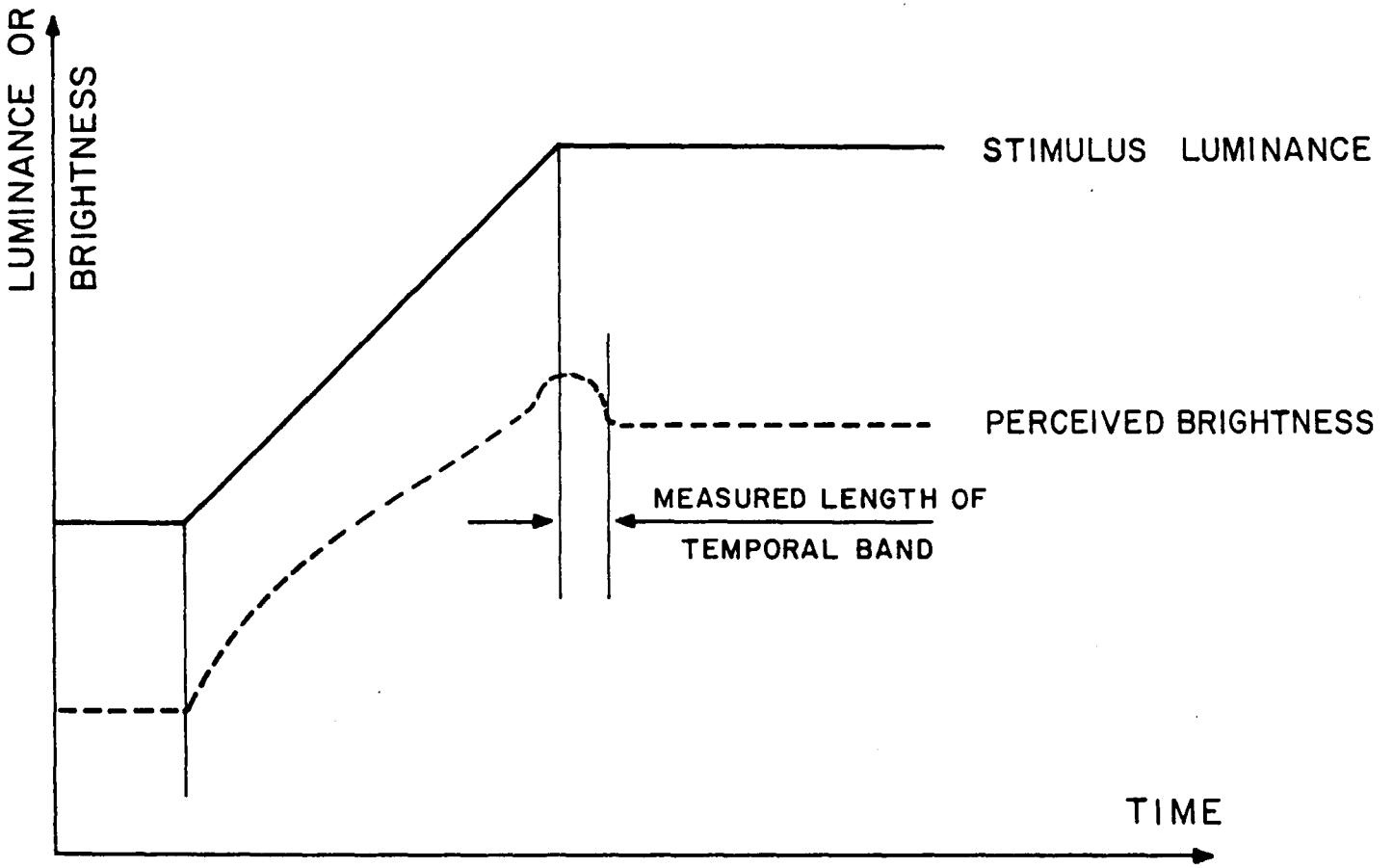

Figure 21. Luminance and perceived brightness of temporal band

and his task was to bring the auditory stimulus in coincidence with the end of the perceived temporal band.

The "personal equation" of some nineteenth century astronomers who were not able to coordinate the visual event of the crossing of a star with the beat of a clock is a classical example of the inability to process simultaneous bi-modal stimuli (Kahneman, 1973).

There are many studies and theories on the subject of divided attention between different sensory mode inputs. These results, often contradictory, show that in split-span experiments, although the task can be performed (Kahneman, 1973), performance is often impaired.

All these experiments deal with only one pair of events that have to be correlated. The events are not repeated.

In the present experiment, however, the pair of events to be correlated is presented repeatedly at regular time intervals, thereby allowing the subject to perform a setting, controlling it himself on the following presentation, and correcting it up to the point where he feels that both events are simultaneous. The task is facilitated by the presentation of the stimulus at equal time intervals, which allows the subject to anticipate its coming and set the sound accordingly.

The trapezoidal time varying stimulus is characterized by the following parameters:

(1) Slope. In order to assess the importance of the slope on the temporal bands, three different slopes were used: 300

msec, 450 msec, and 600 msec (time between the lower and upper level of the trapezoid). The 300 msec was chosen as being greater than the delay time of the pupillary reflex, the 600 msec as being the longest slope at which the temporal bands are perceived reliably by every subject.

(2) Luminance. The maximum linear range of the display was divided into three levels: 20 tr, 220 tr, and 420 tr.

Between those three levels two trapezoidal stimuli were displayed.

The three slopes used can be expressed as 333 tr/sec, 445 tr/sec, and 667 tr/sec (Figure 22).

(3) Presentation rate. A rate of 0.25 Hz was chosen as a constant presentation rate (period of trapezoidal wave is 4 sec) because it is slow enough to permit a good judgement, yet fast enough to permit anticipation and assist in the setting of the controlled stimulus.

The six points to be measured by the subjects are shown in Figure 22.

From the same figure it can be seen that one upper band (5) and one lower band (1) are placed on the same luminance level. The purpose of this design is to check whether there is some intrinsic difference between the upper and lower bands or if the difference is due only to luminance levels. At each of the six points, ten trials were performed, five starting with the auditory stimulus before the temporal band to

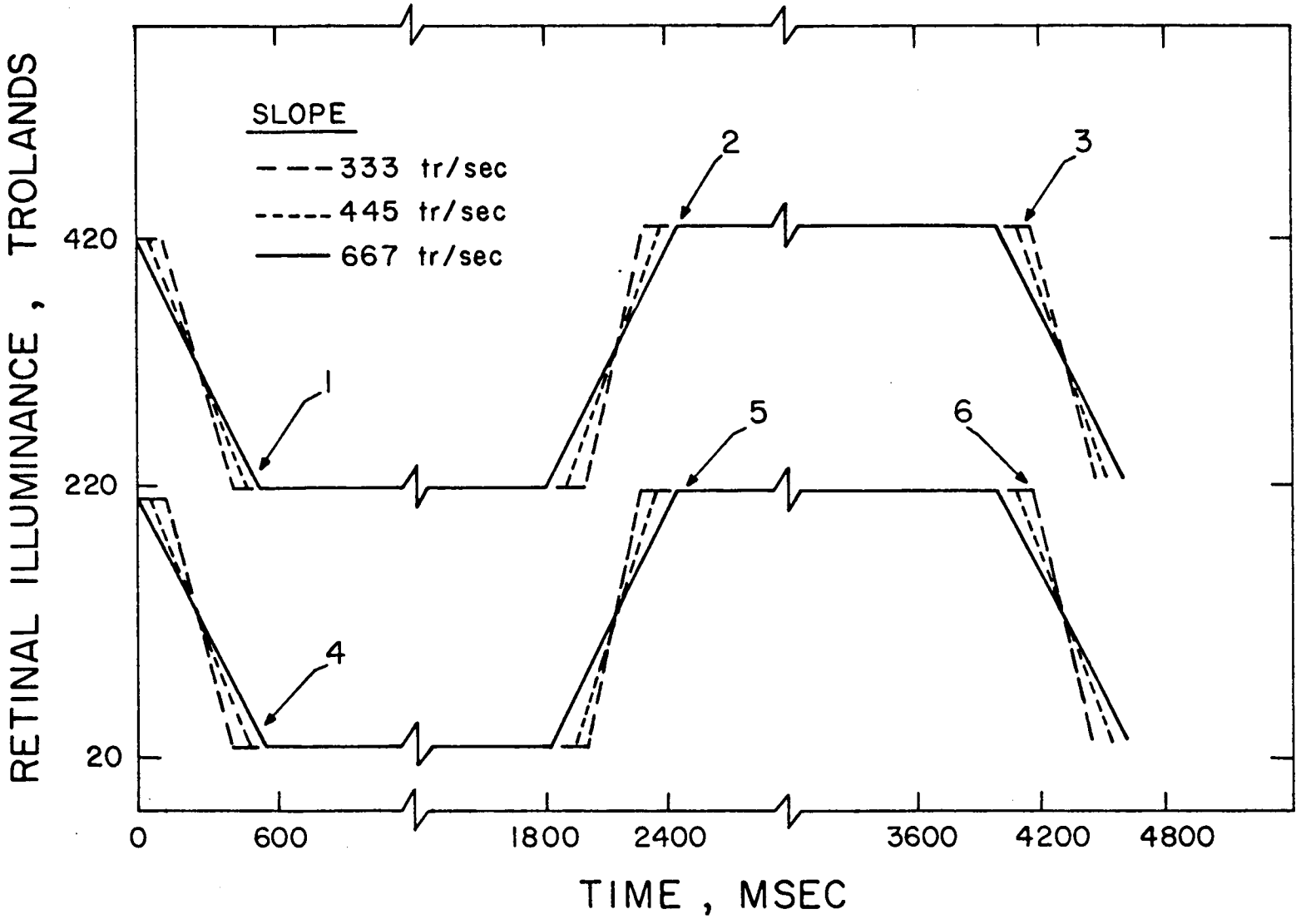

Figure 22. Stimulus waveforms for temporal bands experiments

be measured and requiring the subject to delay it until it comes to coincidence, and five starting from a position after the visual stimulus.

The mean delay time setting of one pair of trials counted as one trial.

The presentation of the three slopes and six measured points was randomized among the 180 trials.

The experimental setup can be seen in Figure 23.

Because of the difficulty of this task, training sessions were conducted for about one hour before starting the experiments. In the training session the subjects were presented with a square wave stimulus and were asked to make the auditory signal coincide with the jump in luminance (dark-bright or bright-dark). At the beginning they were informed of their setting error after each trial. At the end of the training session, two series of ten trials, one for dark-bright and one for bright-dark, were performed and the results recorded. The results show clearly that the subjects are able to perform this task.

At the beginning of each experimental session there was a 5-min adaptation period. The first two trials were discarded.

The experimenter set the slope and luminance, and asked the subject to begin the trial from a delayed or advanced position as per the randomized design. During the time the subject was searching for the coincidence position, the experimenter observed his progress through the oscilloscope.

Figure 23. Photograph of equipment for temporal bands experiment.

When the subject announced he had made a good setting, the experimenter froze the resulting picture in the memory oscilloscope (Figure 19), recorded the length of the temporal band, and set the conditions for the next trial.

From time to time it was observed by the experimenter that the search became erratic; when this happened a 5-min break was taken.

RESULTS

Integration Time Distribution

Of the ten subjects, nine had completely similar answers at all three stages of the experiment. The tenth, an amblyope, did not see the rotating noise, which supports the proposed model.

At the first stage, all nine subjects saw the noise "rotating"; the direction of rotation was determined by the position of the neutral density filter in front of the left or right eye.

For the second stage, the description of how fast they perceived the noise rotating after moving the fixation point in the region covered by the neutral density filter varied between "immediate" to a "fraction of a second".

In the third stage, all nine subjects saw the noise turning *simultaneously* in *both* directions. In the left part of the visual field the noise turned in the direction characterized by "right eye through neutral density filter, left eye unfiltered". In the right part of the visual field, the noise turned in the opposite direction, characterized by "left eye through neutral density filter, right eye unfiltered".

These results show that control of the integration time is a fast adaptation process and that the two halves of the retina can work *simultaneously* at different integration times. These results strongly indicate that the integration time is *locally* controlled in every point of the retina.

Flicker Experiments

Tables A-1 through A-5 in the Appendix contain the raw data of the five subjects.

In Figures 24 through 28 are plotted the means of the modulation at flicker/fusion threshold as a function of frequency.

Four out of the five subjects show the same general form of the curve; the data of the fifth subject, D.S., show the same orderly characteristic form at the low and high frequencies. In the region of the minimum modulation, however, the data from subject D.S. show little correlation to the other subjects data, or to data from classical CFF curves. For some unexplained reason, CFF data for this subject were simply erratic in the most sensitive region.

The high frequency part of the curves is in complete agreement with De Lange's and Kelly's results. For lower frequencies, as predicted by the model, the threshold modulation continues to increase for frequencies lower than 1 Hz. At 0.01 Hz, the curves have still not reached an asymptotic value.

The results show large inter-subject differences in minimum modulation (sensitivity at peak) and in the frequencies at which this minimum modulation (maximum sensitivity) is reached.

The peaks of the curves lie in range of 6 Hz to 18 Hz, which would be translated, if the proposed model is true, to integration times between approximately 84 msec and 30 msec (e.g. a frequency of 6 Hz has a wavelength of approximately 168 msec; the integration time equals half the wavelength or 84 msec).

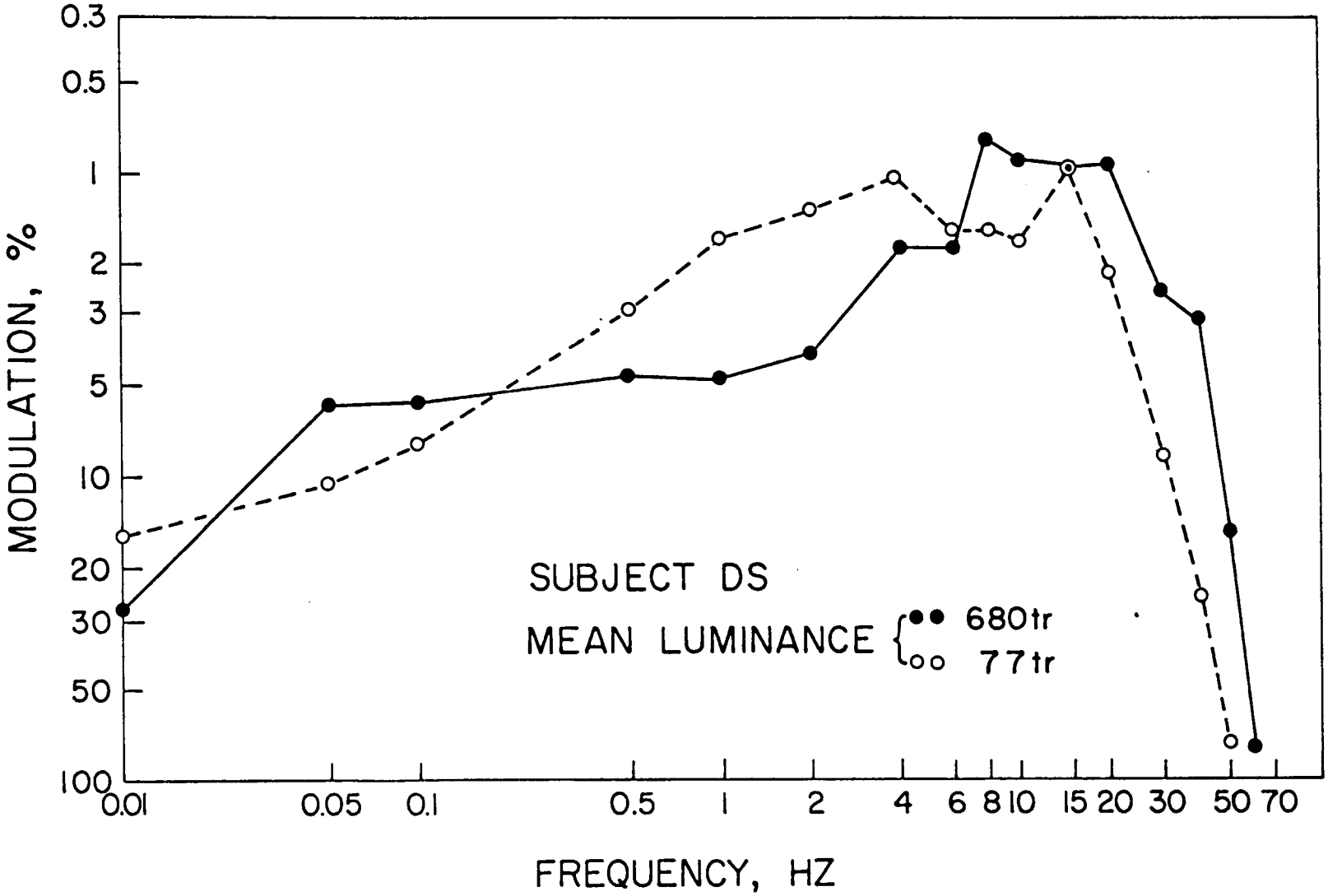

Figure 24. Flicker sensitivity curves, subject DS

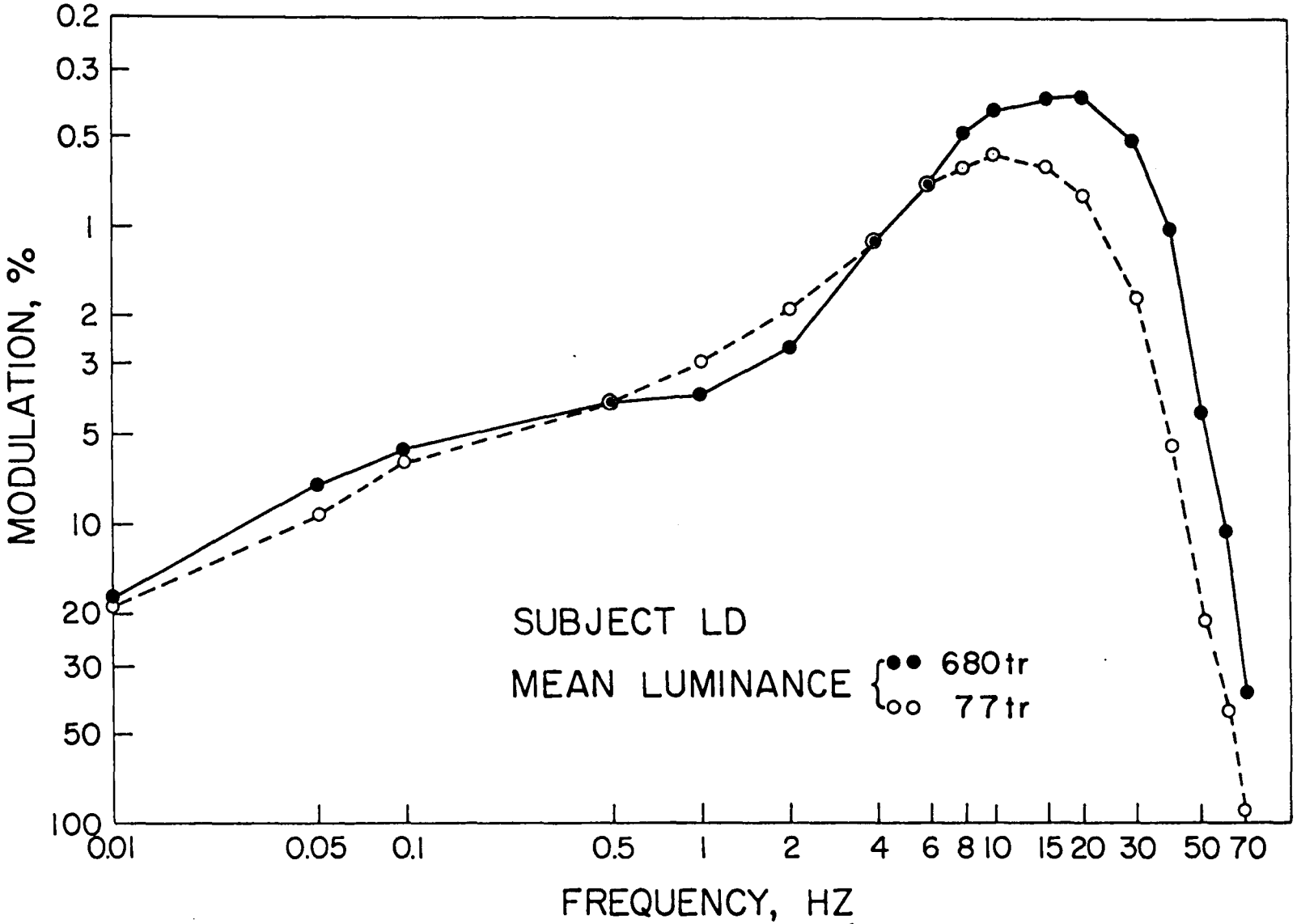

Figure 25. Flicker sensitivity curves, subject LD

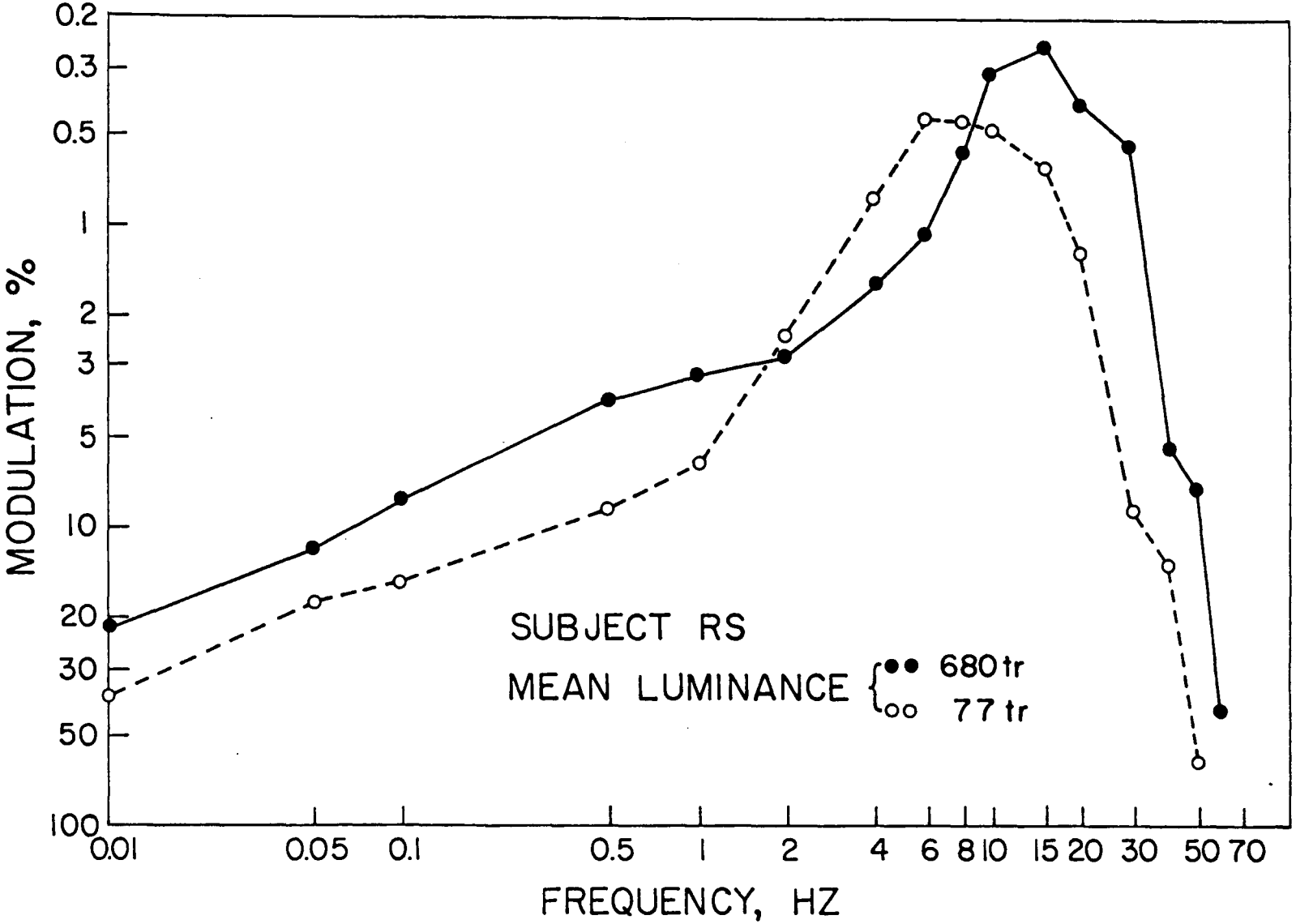

Figure 26. Flicker sensitivity curves, subject RS

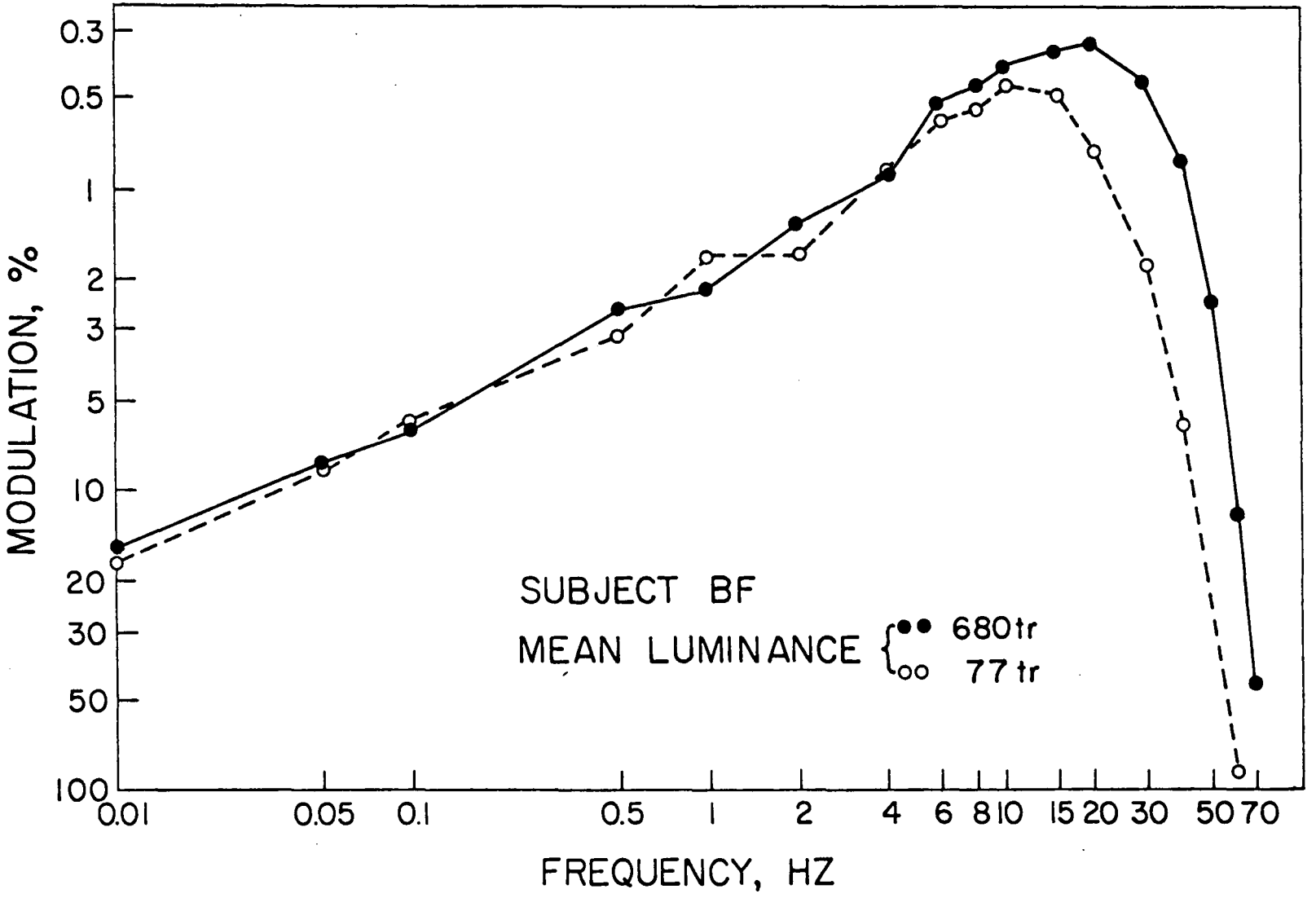

Figure 27. Flicker sensitivity curves, subject BF

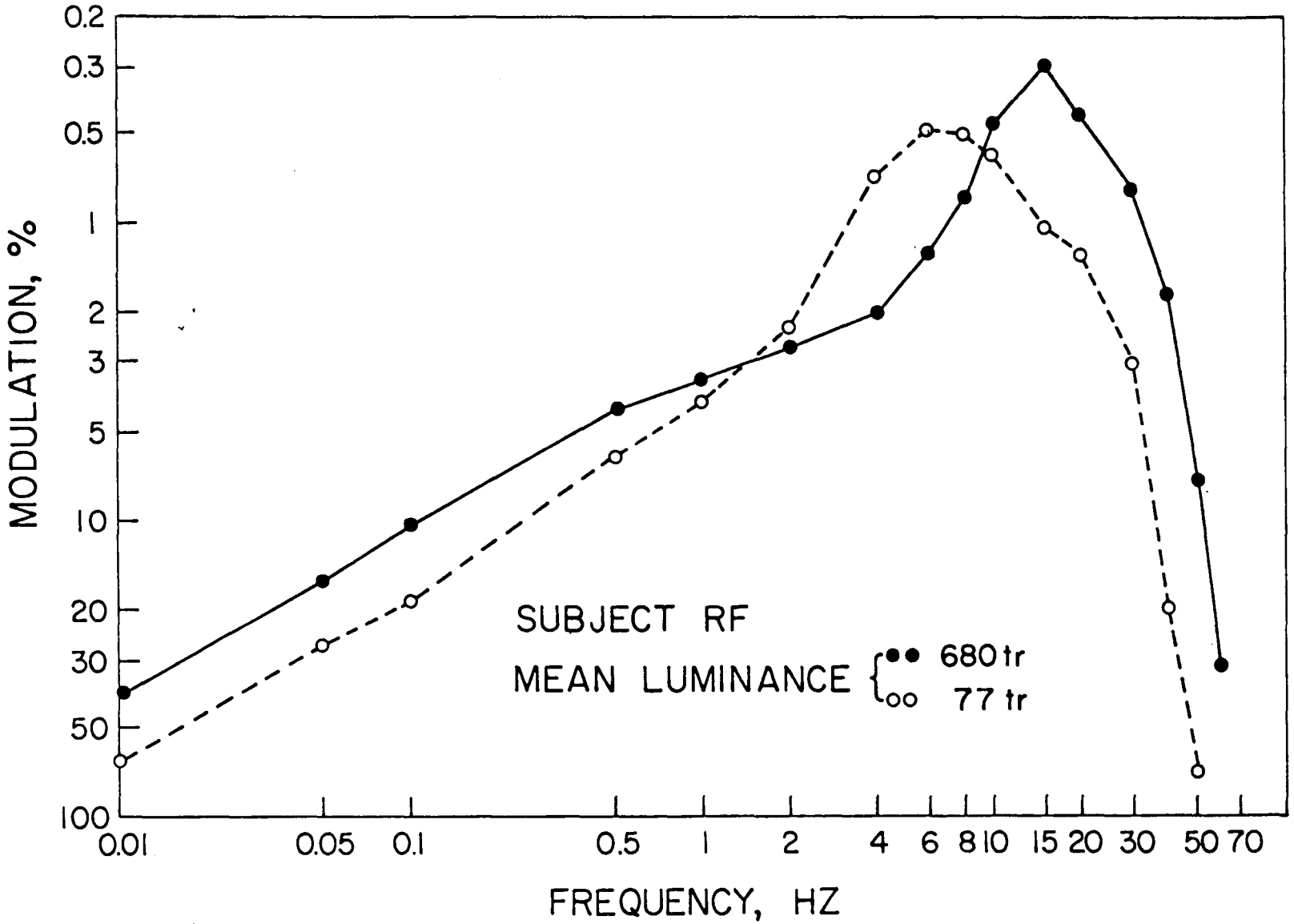

Figure 28. Flicker sensitivity curves, subject RF

No statistical analyses of the data were performed because of the large differences among subjects (which point to intrinsic, organic, individual characteristics) on one hand and the small number of trials per subject combined with the complicated shape of the curves on the other. The general similarities of the curves among subjects are self-evident.

As the mean luminance increases, the peak sensitivity (modulation) increases and the curves are shifted towards higher frequencies. These results agree perfectly with those of Kelly, De Lange, and others. There appears to be a correlation (Figure 29) between the peak frequency (integration time) and sensitivity at that peak frequency across subjects for the same experimental condition. That is, subjects having a lower frequency peak (longer integration time) are more sensitive than subjects showing a shorter integration time (higher frequency peak). This point will be discussed subsequently.

Temporal Bands Experiment

The data for the five subjects are shown in Tables A-6 through A-10 in the Appendix.

In order to check whether the pupillary reflex is a factor in the perception of the temporal bands, all subjects used in the flicker tests were asked if they perceived the temporal bands while their pupils were dilated.

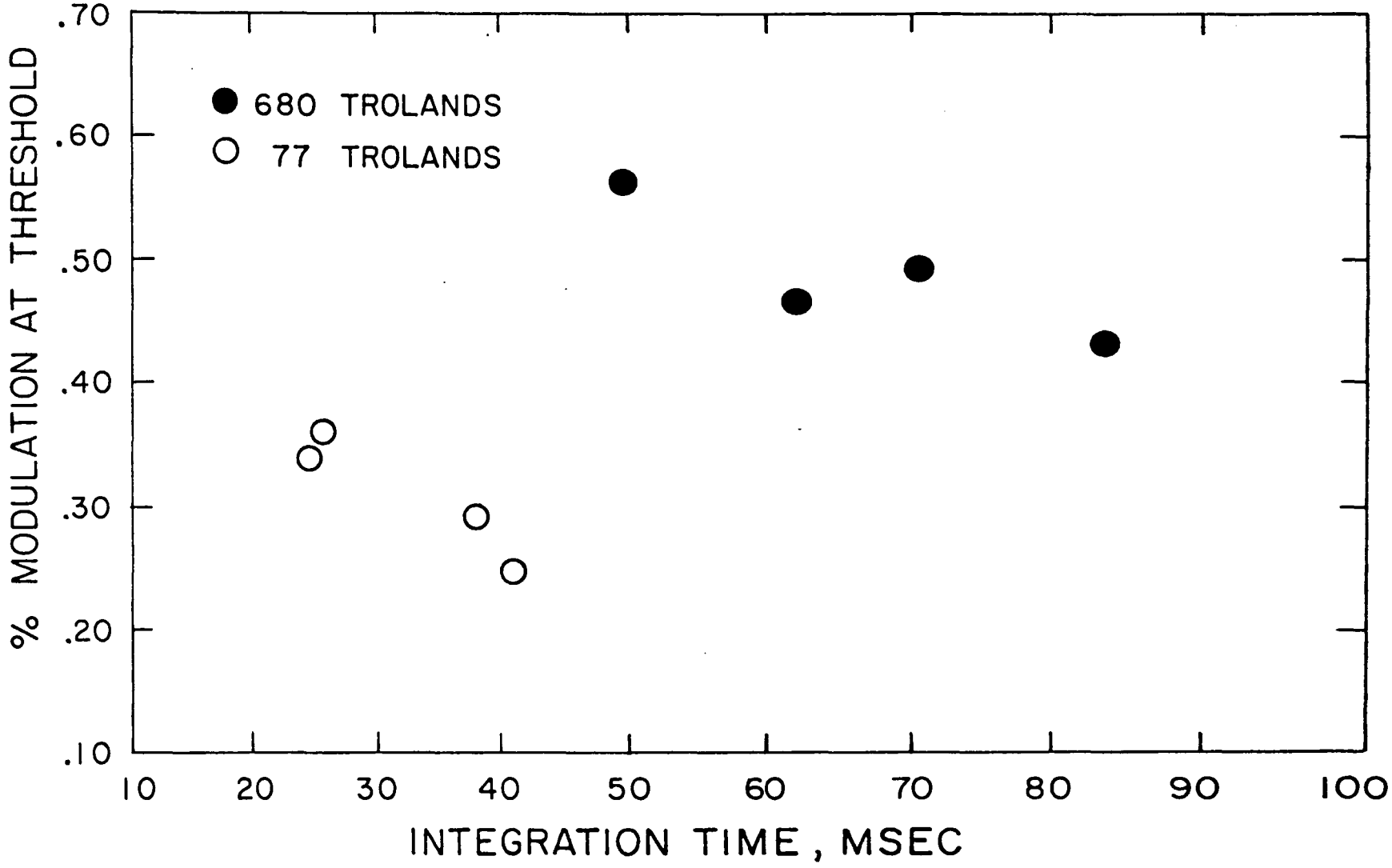

Figure 29. Integration time vs. modulation at frequency of maximum sensitivity; four subjects

One of the subjects (MM) performed two series of temporal band trials, one with dilated pupils and one without. No qualitative differences were found between dilated and nondilated conditions. One can thus conclude that the pupillary reflex is not a determining factor in the creation of the temporal bands. It was therefore decided to perform the temporal band experiments with an active pupillary reflex (normal vision).

The following statistical analyses were performed.

(1) To evaluate the effect of the slope of the luminance trapezoidal waveform, a separate one-way analysis of variance was conducted on the length of the temporal band at each of the six waveform points for every subject. Refer to Figure 21 for the six measured waveform points.

The *F*-test was nonsignificant ($p > .05$) for all points and for all subjects (Table 5), which shows that the slope is not a significant factor in determining the length of the temporal bands.

Subjectively, all observers described the upper temporal band as brighter and, in general, the temporal bands easier to perceive with increasing slope. These subjective descriptions support the idea that the amplitude of the bands is determined largely by the slope, although the lengths of the bands are unaffected by the slopes.

(2) By experimental design, waveform points 1 and 4, 2 and 5, and 3 and 6 are the same type of temporal band (lower band, upper band, and back porch, respectively) differing only by luminance levels.

Table 5. Length of the Temporal Bands and Summary Statistics, by Subjects.

Subject		Waveform Measuring Point 1	2	3	4	5	6
	Length, msec	99.86	40.5	35.8	157.7	98.17	56.8
	S.D.	9.9	14.56	13.5	14.4	8	10.6
	F_{slope}	1.33	0.08	0.42	0.40	0.28	0.84
B.F.	t_{1-4}	-12.10					
	t_{2-5}	-12.25					
	t_{3-6}	- 4.60					
	t_{1-5}	0.51					
	Length, msec	147.5	126.8	97.2	189.0	151.7	127.7
	S.D.	9.55	13.02	14.40	8.75	9.66	31.93
	F_{slope}	0.76	0.03	1.91	1.40	0.43	3.53
R.S.	t_{1-4}	-11.45					
	t_{2-5}	- 5.75					
	t_{3-6}	- 3.30					
	t_{1-5}	- 1.04					
	Length, msec	66.8	33.0	45.0	103.2	63.5	72.3
	S.D.	15.01	5.52	4.72	8.55	5.16	6.40
	F_{slope}	0.21	1.09	0.52	1.41	0.84	0.42
M.M.	t_{1-4}	- 7.80					
	t_{2-5}	-14.06					
	t_{3-6}	- 7.62					
	t_{1-5}	0.77					
	Length, msec	102.6	68.3	51.3	196.2	100.5	60.5
	S.D.	9.55	13.05	13.21	14.05	12.20	11.80
	F_{slope}	0.66	1.50	0.43	1.51	1.76	0.93
B.M.	t_{1-4}	-19.70					
	t_{2-5}	- 6.75					
	t_{3-6}	- 2.23					
	t_{1-5}	0.50					

Table 5. (Continued)

Subject		Waveform Measuring Point 1	2	3	4	5	6
	Length, msec	59.1	43.3	48.2	109.2	59.2	59
	S.D.	4.8	7.4	8.6	11.8	5.6	5.9
	F_{slope}	0.18	0.18	0.03	0.72	1.48	0.27
D.S.	t_{1-4}	-14.70					
	t_{2-5}	- 6.38					
	t_{3-6}	- 3.90					
	t_{1-5}	0.05					

To check whether the luminance is a determining factor in the length of the temporal bands, a t-test was performed for every measured point and subject, pooling data over slopes.

The obtained t-values vary between 2.23 and 19.70, all of which are significant at the 0.05 level of confidence. Thus, luminance is a consistently significant factor in the length of the temporal bands. The results of these t-tests are also summarized in Table 5.

(3) Waveform points 1 and 5 are situated at the same luminance level, but point 1 is a low temporal band and point 5 is a high temporal band.

To check whether there is some intrinsic functional difference between those points, a t-test was also performed on these points for every subject, pooling data across slopes.

The calculated t-values (Table 5) range between 0.05 and 1.04; none is significant at the 0.05 level, again supporting the idea that only the luminance is a significant factor in the length of the temporal bands.

Summary of Results

The integration time is locally controlled on the retina and its dynamics are very fast.

The experimental CFF curves support the proposed temporal model. As the display luminance increases, the temporal frequency at which the eye is most sensitive increases (Figures 24 through 28), indicating that integration time decreases.

Similarly, the length of the temporal bands decreases with increasing luminance (Table 5) from which follows the conclusion that there is a correlation between integration time and the length of the temporal bands.

DISCUSSION

The primary objective of the experimental part of this research was the validation of the proposed temporal model. To that end, three experiments were conducted and their results are totally consistent with the proposed model.

Spatial and temporal integration work together as a fast adaptation system and seem to play a central role in the visual system, a role which is almost neglected in the existing theories about vision.

As predicted by the model, it seems that there is a correlation between the integration time of different observers, their threshold sensitivity, and the length of the temporal band perceived. In order to further evaluate this notion, a brief flicker experiment was performed with the three subjects showing extreme values of temporal bands (M.M., 66.8 msec; D.S., 59 msec; and R.S., 149 msec). The experiment was conducted at 220 tr under the same conditions as in the flicker experiment. The subjects' pupils were not dilated because the frequencies used were from 4 to 16 Hz, where the pupillary reflex is controlled by the mean luminance. The results can be seen in Table 6.

The modulation of maximum sensitivity of R.S. (0.31) is almost half the modulation needed by M.M. and D.S. (0.70 and 0.55, respectively). The peak sensitivity of R.S. lies around 8 Hz which, if the model is valid, can be translated into an integration time of 63 msec. For D.S. this value is 14 Hz (36 msec) and for M.M. 16 Hz

Table 6. Flicker Modulation Thresholds, %, for Illuminance of 220 tr.

Subject		Frequency, Hz							
		4	6	8	10	12	14	16	18
R.S.	Mean	0.80	0.40	0.31	0.33	0.57	0.81		
	S.D.	0.10	0.11	0.07	0.06	0.07	0.26		
D.S.	Mean		1.22	0.85	0.72	0.62	0.55	0.76	
	S.D.		0.16	0.06	0.06	0.06	0.08	0.09	
M.M.	Mean		0.96	0.76	0.89	0.77	0.72	0.70	0.73
	S.D.		0.10	0.09	0.17	0.09	0.20	0.08	0.11

(32 msec).

The temporal bands at this luminance are 149 msec for R.S., 59 msec for D.S., and 66.8 msec for M.M.

If the proposed model is valid, the temporal band should be perceived at double the integration time and the modulation at the maximum sensitivity frequency of R.S. should be about half the modulation of D.S. and M.M. This prediction is very accurate as can be seen from the ratio of the actual temporal bands and integration time, which were 2.36 for R.S., 1.63 for D.S., and 2.09 for M.M. (The model predicts a ratio of 2). The ratios of the modulation at the maximum sensitivity of R.S. to those of M.M. and D.S. were 0.44 and 0.56, respectively. The model predicts a ratio of 0.51 for the former and 0.57 for the latter.

Although there is not enough statistical evidence to fully prove the model, the existing data are extremely encouraging. Further research to gather enough data for a complete statistical analysis is strongly recommended.

In addition, some anecdotal evidence is interesting. The two subjects having short integration times expressed a need to use more light than normal at their working place, while the subject having a long integration time and the author, who also has a measured long integration time, work with a minimum amount of light at their work place. These facts suggest a very strong relationship between spatial and temporal encoding.

The hypothesis about temporal and spatial control of the integration time can provide the mechanism through which lateral inhibition manifests itself, and can explain the spatial Mach bands not only in their general form but also in the assymetry between the dark and bright Mach bands.

It is known that the dark Mach band is larger than the bright band. Because of the lower luminance in the dark part of the Mach pattern, more retinal sensors are summed together through spatial summation, enlarging the area on which the lateral inhibition through temporal integration works, making the dark band larger.

As reported by Fiorentini and Radici (from Ratliff, 1965) the width of the bands seems to be a function of the pattern's slope, decreasing with increasing slopes, and disappearing for abrupt steps. The disappearance at abrupt steps is probably caused by both bands being summed together and therefore cancelling one another. As for the change in width with slope, the explanation can probably be found in the way the stimulus is generated. The change in slope is produced by varying the distance between the constant uniform dark and bright fields. As reported by Mach (Ratliff, 1965) there is a finite distance (16 min of arc) at which lateral inhibition takes place.

In the proposed model, this finite distance varies with luminance. The distances used in Fiorentini and Radici's (from Ratliff, 1965) experiments vary between 10 to 50 min of arc; they are of the same order of magnitude as the finite lateral inhibition width and therefore can provide the explanation of the changes in the width of

the bands with slope.

Backwards masking can also be explained by the present model. A visual event, the mask, coming after the stimulus to be detected can change the value of the integration time while the stimulus "travels" through the integrators. The change in integration time changes the value of the output of the integrators and therefore affects the perception (detection) of the stimulus.

The temporal bands also explain the Broca-Sulzer effect. Pulses of light are perceived brighter if their length equals the integration time; shorter or longer pulses are perceived as less bright. The temporal band (which lasts for one integration period) will add maximum brightness to pulses of the same length. Longer pulses will be perceived at their true value (no remaining temporal band beyond the integration time at the end of the pulse), creating the illusion that longer pulses are dimmer than shorter ones.

From the harmonic analysis of periodic functions, it is known that a periodic function $F(t)$ can be represented by a Fourier series only when an infinite number of factors is summed. When the sum contains only a finite number of factors, the representation of $F(t)$ shows an oscillation around the discontinuity points. This is termed the Gibbs phenomenon (Stuart, 1961). For a square wave, the Gibbs oscillation is shown in Figure 30.

At first glance the Fourier analysis approach looks like a good explanation for the temporal bands (Ratliff, 1965). The eye seems to perform as a Fourier analyzer. Due to the limited MTF, however, only

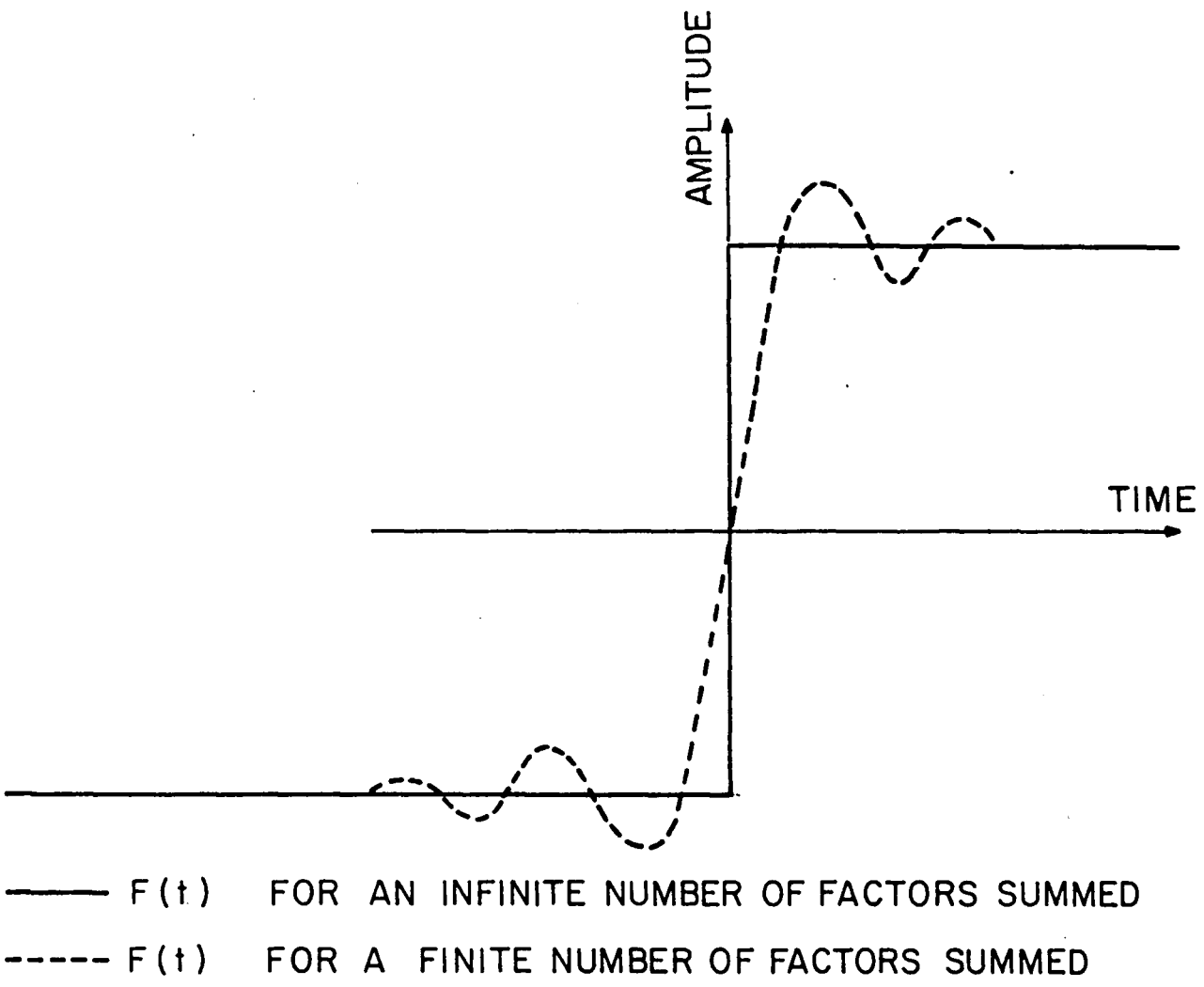

Figure 30. Gibbs oscillation for finite number of factors

a small number of frequencies is summed, thus theoretically leading to the Gibbs phenomenon.

More careful study shows that the temporal bands are not produced as predicted by the Gibbs phenomenon. That is,

(1) No ringing was observed; and

(2) The low and high bands are not symmetrical.

Moreover, the absence of the Gibbs ringing in the temporal and spatial perception of discontinuities proves that the eye does not work exactly as a Fourier analyzer.

In general, it seems that the integration of time and space are very basic, individual characteristics, and as such, might be the controlling factors in other simple and complex skills involving the visual system. Further exploration of this concept into the general realm of individual differences is clearly warranted.

APPLICATIONS OF THIS RESEARCH

The importance of the results obtained in this research lies in the fact that they permit a better understanding of the internal mechanisms in the visual process.

A crude notion of integration time (generally assumed to be constant in time and space) is used in the modern theories about perception of displayed information. The most comprehensive theory, developed by Biberman and Rosell (Biberman, Legault, Rosell, Schade, Schnitzler, Snyder, and Wilson, 1973) states that the signal-to-noise ratio at the display (SNR_D) is a linear function of the square root of the integration time. In a good visual display, a contrast ratio of 40:1 and more is achieved. Depending on the luminance at which the display is set and upon the ambient illuminance, the integration time might vary interscene and intrascene by a factor of at least 2:1 up to 4:1, which can change the value of the SNR_D by as much as 100%. Thus, existing SNR_D approaches require further examination.

A practical application of the results obtained concerns the optimization of the conditions under which information should be displayed. Images of moving targets, with little or no noise, should be seen in bright light in order to keep the integration time and space at a minimum. For example, dynamic cockpit displays ought to be made as bright as possible.

On the other hand, images embedded in noise (low light level T.V., for example) should be looked at in a very dim environment to increase

the integration time and therefore filter out more noise. Because the eye-brain system trades off integration time for integration space, the acuity remains high, while the perceived noise is reduced through increased temporal integration.

EXTENSIONS OF THIS RESEARCH

Future research should be conducted in two directions.

First, consolidation of the present results is desirable by performing a large number of experiments to provide a good statistical basis for the analysis of temporal integration under various viewing conditions.

Secondly, the research field should be enlarged in the following directions:

(1) Quantitative measure of the dynamics of the integration time, to provide the information needed for the building of a better temporal or spatio-temporal model. This quantitative model should be simulated in a digital computer and its output compared to the experimental results for validation purposes.

(2) Extension of the performed experiments to the scotopic range of retinal illumination.

(3) Investigate the relationship between time and spatial integration using moving targets to determine their effect on integration time.

(4) Quantitative study of parallel effects of time delays and integration time to provide a complete proof of the identity of their effects, and therefore consolidate the hypothesis of their identical cause.

(5) Study of possible correlations of integration time with other visual, reading, and motor skills.

(6) Study of possible correlations of the integration time with pathological states of the visual system (amblyopia, *etc.*).

(7) Study of diurnal, age, and other factors influencing the integration time.

(8) Is the integration time a continuous or discrete process? This is a long debated problem, but the apparatus developed in the present research can provide the tool for solving it.

References

Arend, L. E. Response of the human eye to spatially sinusoidal gratings at various exposure durations, *Vision Research*, 1976, *16*, 1311-1315. (a)

Arend, L. E. Temporal determinants of the form of the spatial contrast threshold MTF, *Vision Research*, 1976, *16*, 1035-1042. (b)

Biberman, L. M., Legault, R. R., Rosell, F. A., Schade, D. H., Schnitzler, A. D., Snyder, H. L., and Willson, R. H. *Perception of displayed information*, New York: Plenum, 1973.

Brown, J. L. and Black, J. E. Critical duration for resolution of acuity targets, *Vision Research*, 1976, *16*, 309-315.

Brown, L. T. Flicker and intermitent stimulation, in C. H. Graham (Ed.), *Vision and Visual Perception*, New York: Wiley, 1965.

Brindley, G. S. *Physiology of the retina and visual pathway*, Baltimore: Williams and Wilkins, 1970.

Campbell, F. W. and Robson, J. G. Application of Fourier analysis to the visibility of gratings, *Journal of Physiology*, 1968, *197*, 552-568.

Childress, D. S. and Jones, R. W. Mechanics of horizontal movement of the human eye, *Journal of Physiology*, 1967, *188*, 273-284.

Cornsweet, T. N. and Crane, H. D. Accurate two-dimensional eye tracker using first and fourth purkinje images, *Journal of the Optical Society of America*, 1973, *63*, 921-928.

Ditchburn, R. W. *Eye movements and visual perception*, Oxford: Clarendon Press, 1973.

Graham, C. H. (Ed.) *Vision and visual perception*, New York: Wiley, 1965.

LeGrand, Y. and Geblewicz, E. Recherches sur la vision laterale, *Revue d'Optique*, 1938, *17*, 257-263.

LeGrand, Y. *Les yeux et la vision*, Paris: Dunod, 1960.

deGroot, S. G. and Gebhard, J. W. Pupil rise as determined by adapting luminance, *Journal of the Optical Society of America*, 1952, *42*, 492-495.

Herrick, R. M. Foveal luminance discrimination as a function of the duration of the decrement or increment in luminance, *Journal of Comparative and Physiological Psychology*, 1956, *49*, 438-443.

Kahneman, D. and Norman, J. The time-intensity relation in visual perception as a function of the observer's task, *Journal of Experimental Psychology*, 1964, *68*, 215-220.

Kahneman, D. *Attention and effort*, Englewood Cliffs, New Jersey: Prentice-Hall, 1973

Keesey, U. T. Effect of involuntary eye movements on visual acuity, *Journal of the Optical Society of America*, 1960, *70*, 769-774.

Keesey, U. T. Flicker and patern detection: A comparison of thresholds, *Journal of the Optical Society of America*, 1972, *62*, 446-448.

Keesey, U. T. and Jones, R. M. The effect of micromovements of the eye and exposure duration on contrast sensitivity, *Vision Research*, 1976, *16*, 481-488.

Kelly, D. H. Effects of sharp edges in a flickering field, *Journal of the Optical Society of America*, 1959, *49*, 730-732.

Kelly, D. H. Stimulus patterns for visual research, *Journal of the Optical Society of America*, 1960, *50*, 1115-1117.

Kelly, D. H. Visual responses to time-dependent stimuli: I. Amplitude sensitivity measurements, *Journal of the Optical Society of America*, 1961, *51*, 422-429. (a)

Kelly, D. H. Flicker fusion and harmonic analysis, *Journal of the Optical Society of America*, 1961, *51*, 917-918. (b)

Kelly, D. H. Visual signal generator, *Review of Scientific Instrumentation*, 1961, *32*, 50-55. (c)

Kelly, D. H. Frequency doubling in visual responses, *Journal of the Optical Society of America*, 1966, *56*, 1628-1633.

Kelly, D. H. Diffusion model of linear flicker responses, *Journal of the Optical Society of America*, 1969, *59*, 1665-1670.

Kelly, D. H. Theory of flicker and transient responses, I. Uniform fields, *Journal of the Optical Society of America*, 1971, *61*, 537-546 (a)

Kelly, D. H. Theory of flicker and transient responses, II. Counterphase gratings, *Journal of the Optical Society of America*, 1971, *61*, 632-640. (b)

Kelly, D. H. Adaptation effects on spatiotemporal sine-wave thresholds, *Vision Research*, 1972, *12*, 89-101.

Kelly, D. H. How many bars make a grating?, *Vision Research*, 1975, *15*, 625-626. (a)

Kelly, D. H. Spatial frequency selectivity in the retina, *Vision Research*, 1975, *15*, 665-672. (b)

Kelly, D. H. Pattern detection and the two-dimensional Fourier transform: Flickering checkerboards and chromatic mechanisms, *Vision Research*, 1976, *16*, 277-287.

DeLange, H. Relationship between critical flicker frequency and a set of low-frequency characteristics of the eye, *Journal of the Optical Society of America*, 1954, *44*, 380-389.

DeLange, H. Research into the dynamic nature of the human fovea-cortex systems with intermittent and modulated light, *Journal of the Optical Society of America*, 1958, *48*, 777-784.

DeLange, H. Eye's response at flicker fusion to square-wave modulation of a test field surrounded by a large steady field of equal mean luminance, *Journal of the Optical Society of America*, 1961, *51*, 415-421.

Levinsohn, J. Flicker fusion phenomena, *Science*, 1968, *160*, 21-28.

Nachmias, J. Effect of exposure duration on visual contrast sensitivity with square wave gratings, *Journal of Optical Society of America*, 1967, *57*, 421-247.

Naka, K. I. The horizontal cell, *Vision Research*, 1972, *12*, 537-545.

Ratliff, F. *Mach bands: Quantitative studies on neural networks in the retina*, San Francisco: Holden-Day, 1965.

Remole, A. Subjective patterns in a flickering field: Binocular vs. monocular observation, *Journal of the Optical Society of America*, 1973, *63*, 745-748.

Remole, A. Luminance thresholds for perceived movement in a flickering field, *Journal of the Optical Society of America*, 1974, *64*, 1133-1135.

Rodieck, R. W. *The vertegrate retina*, San Francisco: W. H. Freeman, 1973.

Ross, J. The resources of binocular perception, *Scientific American*, March 1976, *234*, 80-86.

Savoy, R. L. and McCann, J. J. Visibility of low spatial frequency sine-wave targets: Dependence on number of cycles, *Journal of Optical Society of America*, 1975, *65*, 343-350.

Schober, H. A. W. and Hilz, R. Contrast sensitivity of the human eye for square wave gratings, *Journal of Optical Society of America*, 1965, *55*, 1086-1091.

Smythies, J. R. A preliminary analysis of the stroboscopic patterns, *Nature (London)*, 1957, *179*, 523-524.

Sperling, G. and Sondhi, M. M. Model for visual luminance discrimination and flicker detection, *Journal of the Optical Society of America*, 1968, *58*, 1133-1145.

Stevens, S. S. Duration, luminance, and the brightness exponent, *Perception and Psychophysics*, 1966, *1*, 96-100.

Stuart, R. D. *An introduction to Fourier analysis*, New York: Wiley, 1961.

Tynan, P. and Sekuler, R. Perceived spatial frequency varies with stimulus duration, *Journal of the Optical Society of America*, 1974, *64*, 1251-1255.

Van Meeteren, A. *Visual aspects of image intensification*, Technical Report, Soesterberg, Netherlands, Institute for Perception, TNO, 1973.

Veringa, F. Diffusion model of linear flicker responses, *Journal of the Optical Society of America*, 1970, *60*, 285-286.

Watanabe, A., Mori, T., Nagata, S. and Hiwatashi, K. Spatial sine-wave responses of the human visual system, *Vision Research*, 1968, *8*, 1245-1263.

Weale, R. A. Spectral sensitivity and wave-length discrimination of the peripheral retina, *Journal of Physiology*, 1953, *119*, 170-190.

Yarbus, A. L. *Eye movements and vision*, New York: Plenum, 1967.

APPENDIX

RAW EXPERIMENTAL DATA

Table A1. Modulation at Threshold, %.
Subject R.F.

Frequency, Hz	Illuminance, Tr. 77				680			
	Pairs of Trials		Pairs of Trials		Pairs of Trials		Pairs of Trials	
0.01	61.17	72.71	--	--	39.12	38.46	--	--
0.05	26.17	23.87	31.25	24.95	10.75	12.93	23.19	17.83
0.1	16.10	21.22	19.20	19.88	9.15	14.25	11.70	5.92
0.5	6.10	6.20	6.15	6.15	4.15	4.79	4.02	4.40
1	3.82	3.88	4.00	4.34	3.10	3.16	3.00	4.36
2	2.18	1.98	2.08	2.08	2.35	2.59	2.80	2.46
4	0.73	0.77	0.68	0.72	2.15	1.95	2.05	2.13
6	0.51	0.51	0.43	0.49	1.40	1.66	1.00	1.06
8	0.50	0.42	0.58	0.50	1.23	0.83	0.50	0.72
10	0.57	0.57	0.53	0.69	0.50	0.48	0.42	0.56
15	0.77	0.87	1.10	1.32	0.36	0.40	0.18	0.30
20	1.10	1.34	1.45	1.11	0.33	0.33	0.35	0.71
30	2.00	2.92	3.89	2.89	0.71	0.73	0.78	0.74
40	20.00	19.50	19.76	19.76	1.51	1.59	1.90	1.78
50	71.15	72.55	70.03	70.37	7.23	7.23	7.91	7.87
60	--	--	--	--	30.96	29.52	30.18	37.66
70	--	--	--	--	--	--	--	--

- Undetectable flicker at maximum modulation.

Table A2. Modulation at threshold, %.
Subject D.W.

Frequency, Hz	Illuminance, Tr. 77				680			
	Pairs of Trials		Pairs of Trials		Pairs of Trials		Pairs of Trials	
0.01	18.05	18.47	--	--	16.55	17.65	--	--
0.05	9.22	9.26	9.24	9.24	7.10	7.36	7.30	6.64
0.1	6.27	6.27	6.35	6.23	5.52	5.52	5.40	5.90
0.5	3.40	3.64	4.71	4.53	4.08	4.08	4.15	3.21
1	3.18	3.66	2.35	2.35	3.80	4.10	3.71	3.39
2	1.51	1.47	1.89	2.71	2.70	2.56	2.45	2.45
4	1.10	1.10	1.18	1.24	1.08	1.24	1.07	1.07
6	0.88	0.84	0.60	0.68	0.78	0.78	0.63	0.81
8	0.67	0.69	0.60	0.60	0.51	0.61	0.40	0.44
10	0.57	0.57	0.57	0.57	0.31	0.41	0.38	0.52
15	0.55	0.56	0.67	0.68	0.37	0.38	0.31	0.42
20	0.76	0.75	0.83	0.81	0.35	0.65	0.15	0.25
30	1.71	1.72	1.70	1.71	0.47	0.49	0.47	0.57
40	5.27	5.28	5.28	5.29	0.87	0.91	1.01	1.08
50	20.17	21.18	19.85	23.26	4.42	4.51	4.08	4.08
60	41.17	45.06	43.21	38.63	10.17	10.86	10.23	10.28
70	91.20	95.13	89.17	91.25	35.18	37.14	39.25	33.01

Table A3. Modulation at threshold, %.
Subject B.F.

Frequency, Hz	Illuminance, Tr. 77				680			
	Pairs of Trials		Pairs of Trials		Pairs of Trials		Pairs of Trials	
0.01	16.01	16.90	--	--	14.18	16.31	--	--
0.05	8.31	8.36	9.11	9.32	7.55	8.24	8.38	8.46
0.1	5.80	6.06	6.07	6.08	6.53	6.62	6.18	6.18
0.5	3.00	3.01	3.18	3.57	2.42	2.43	2.53	2.80
1	1.57	1.66	1.88	1.89	2.08	2.11	2.32	2.42
2	1.48	1.49	1.59	2.05	1.38	1.39	1.28	1.28
4	0.83	0.84	0.85	0.91	0.95	0.98	0.85	0.79
6	0.38	0.47	0.83	0.86	0.52	0.53	0.54	0.53
8	0.55	0.55	0.56	0.59	0.48	0.45	0.46	0.47
10	0.37	0.39	0.47	0.53	0.48	0.36	0.41	0.40
15	0.48	0.47	0.49	0.46	0.34	0.35	0.35	0.36
20	0.75	0.75	0.75	0.75	0.34	0.29	0.31	0.37
30	1.80	1.82	1.83	1.84	0.34	0.34	0.41	0.63
40	5.70	6.23	7.12	8.34	0.79	0.80	0.72	0.88
50	27.33	29.75	30.07	35.79	2.38	2.43	2.51	2.37
60	85.50	89.38	91.17	92.23	12.10	12.41	13.53	11.47
70	--	--	--	--	43.12	39.68	48.02	48.19

- Undetectable flicker at maximum modulation.

Table A4. Modulation at threshold, %.
Subject R.S.

Frequency, Hz	Illuminance, Tr. 77				680			
	Pairs of Trials		Pairs of Trials		Pairs of Trials		Pairs of Trials	
0.01	35.17	40.01	--	--	18.15	22.86	--	--
0.05	18.05	18.83	17.85	16.83	11.25	10.86	12.09	12.10
0.1	15.58	15.58	15.38	12.95	7.83	9.02	7.34	8.18
0.5	8.70	8.85	8.84	8.55	3.79	3.47	3.90	3.99
1	5.80	5.93	5.95	5.97	3.10	3.11	3.20	3.21
2	2.28	2.28	2.28	2.28	2.40	2.61	2.91	3.09
4	0.70	0.81	0.89	0.97	1.53	1.57	1.56	1.53
6	0.48	0.39	0.38	0.47	1.01	1.06	1.03	1.04
8	0.39	0.47	0.49	0.45	0.56	0.56	0.52	0.59
10	0.53	0.49	0.45	0.38	0.30	0.31	0.30	0.33
15	0.58	0.65	0.65	0.63	0.24	0.25	0.25	0.25
20	1.39	1.21	1.08	1.15	0.41	0.22	0.45	0.44
30	8.32	8.81	8.70	8.86	0.39	0.46	0.55	0.71
40	14.09	13.22	12.50	12.51	1.29	1.45	1.83	1.60
50	60.15	66.71	65.12	62.61	6.11	7.32	7.45	8.31
60	--	--	--	--	42.05	39.90	39.01	39.23
70	--	--	--	--	--	--	--	--

- Undetectable flicker at maximum modulation.

Table A5. Modulation at Threshold, %,
Subject D.S.

Frequency, Hz	Illuminance, Tr. 77				680			
	Pairs of Trials		Pairs of Trials		Pairs of Trials		Pairs of Trials	
0.01	13.78	17.82	--	--	23.17	32.07	--	--
0.05	10.19	14.39	7.15	9.09	5.40	5.91	5.72	5.86
0.1	7.05	8.31	9.12	6.24	5.01	5.00	5.89	6.47
0.5	2.45	2.80	2.85	2.85	4.23	5.37	4.15	4.32
1	1.58	1.62	1.59	1.60	4.29	4.65	4.33	5.41
2	1.10	1.19	1.35	1.56	3.32	2.46	4.83	5.17
4	1.01	1.03	1.05	0.99	1.83	2.11	1.42	1.70
6	1.43	1.11	1.89	1.53	1.46	1.71	1.79	1.90
8	1.20	1.35	1.85	1.66	0.75	0.77	0.76	0.76
10	1.63	1.67	1.71	1.80	0.74	0.77	0.92	1.09
15	1.00	1.01	0.95	0.90	0.95	0.95	0.96	0.99
20	2.18	2.31	2.00	1.93	0.88	0.89	0.93	0.97
30	8.18	8.94	7.38	10.39	2.18	2.54	2.56	2.56
40	18.73	24.29	29.18	26.14	2.51	3.02	3.15	3.69
50	63.19	76.81	81.32	88.68	12.92	16.54	14.19	16.31
60	--	--	--	--	63.15	76.85	82.24	87.76
70	--	--	--	--	--	--	--	--

- Undetectable flicker at maximum modulation.

Table A6. Temporal Bands
Subject M.M.

Preliminary Trials: Delays, msec

Dark to Bright	-30	30	0	5	0	0	0	0	5	10
Bright to Dark	-30	0	20	-15	10	30	30	20	0	0

Length of the Temporal Bands, msec

Measuring Point	Slope, msec 600		450		300	
1	80-60,* 80-40, 65-50	90-70 65-60	60-80, 70-60, 70-50	50-85 60-45	160-70, 40-65, 60-40	120-10 60-70
2	40-10, 20-40, 30-30	55-15 20-40	50-40, 50-10, 30-35	30-25 30-40	40-35, 50-10, 40-45	25-30 40-35
3	40-55, 40-40, 60-50	60-40 40-60	45-60, 50-30, 55-35	45-40 45-40	55-65, 60-30, 40-45	35-45 35-50
4	80-120, 80-105, 120-100	80-90 120-95	120-100, 90-105, 105-110	140-90 100-120	110-80, 120-100, 105-120	100-90 90-110
5	90-30, 65-55, 70-70	60-50 70-60	100-20, 90-40, 40-70	80-40 40-100	80-70, 100-40, 70-45	40-80 80-60
6	60-80, 60-100, 65-60	70-80 70-70	70-90, 65-60, 80-80	80-70 70-80	70-70, 60-60, 80-75	70-70 85-70

*Pairs of trials, first trial ascending in delay time, second trial descending in delay time.

Table A7. Temporal Bands
Subject B.M.

Preliminary Trials Delays, msec

Dark to Bright	15	30	-20	-5	-5	30	35	40	25	15
Bright to Dark	-20	30	20	40	10					

Length of the Temporal Bands, msec

Measuring Point	Slope, msec 600		450		300	
1	140-70,* 100-120, 65-105	130-65 180-10	140-60, 120-100, 60-90	180-60 140-80	145-65, 115-90, 125-85	155-70 105-100
2	60-70, 40-110, -10-80	0-125 70-60	80-60, 100-45, 105-15	80-70 -10-200	80-80, 10-105, 125-85	100-20 100-60
3	0-65, 45-100, 20-90	-10-95 70-60	35-50, 20-45, 0-105	65-25 80-40	25-65, 120-20, 70-0	40-60 65-75
4	220-140, 230-160, 200-180	200-180 200-170	200-200, 230-180, 200-210	210-180 220-190	200-165, 260-200, 175-245	260-85 180-205
5	120-40, 140-40, 120-70	160-40 180-40	120-105, 120-60, 100-120	90-85 115-65	130-80, 100-95, 90-125	145-60 160-100
6	60-60, 45-70, 60-80	60-40 45-125	70-65, 25-80, 45-90	15-95 70-70	85-55, -10-80, 0-90	40-75 120-10

*Pairs of trials, first trial ascending in delay time, second trial descending in delay time.

Table A8. Temporal Bands
Subject B.F.

Preliminary Trials Delays, msec

Dark to Bright	40	25	-30	-40	0	45	25	30	-10	30
Bright to Dark	100	-20	25	45	30	-15	0	80	-75	20

Length of the Temporal Bands, msec

Measuring Point	Slope, msec 600		450		300	
1	105-105,* 105-50, 105-100	150-45 135-100	115-95, 145-30, 80-135	125-35 105-100	175-45, 130-75, 75-120	100-120 105-100
2	Subject Does Not See the Band Reliable		65-40, 60-70, 0-35	-10-75 35-50	20-60, 30-35, 0-55	65-60 20-45
3	100-20, 45-45, 45-20	35-50 15-45	15-90, 0-60, 45-35	45-30 65-0	45-0, 35-50, 40-55	-10-0 5-90
4	100-225, 145-170, 100-192	125-195 125-155	165-200, 135-190, 135-170	140-195 105-185	180-115, 155-160, 200-145	165-95 175-190
5	70-115, 105-90, 95-105	95-120 75-95	80-115, 55-170, 100-105	110-75 10-155	65-130, 100-100, 115-100	130-80 35-150
6	50-20, 45-75, -10-95	0-135 60-65	145-0, -10-115, 90-35	65-45 55-80	55-45, 50-50, 45-100	35-60 -10-120

*Pairs of trials, first trial ascending in delay time, second trial descending in delay time.

Table A9. Temporal Bands
Subject D.S.

Preliminary Trials Delays, msec

Dark to Bright	0	-25	-5	15	20	-5	0	10	0	-5
Bright to Dark	15	25	0	-10	-5	20	15	-5	0	5

Length of the Temporal Bands, msec

Measuring Point	Slope, msec 600		450		300	
1	45-85, 80-40, 65-55	35-80* 45-70	45-65, 100-35, 35-65	70-40 80-45	55-60, 90-45, 60-60	20-90 45-65
2	45-40, 65-10, 0-85	80-5 40-50	45-50, -5-80, -5-95	0-75 50-45	45-40, 30-50, 50-10	55-40 30-100
3	65-70, 30-55, 45-40	40-55 30-35	50-45, 70-25, 0-75	60-55 60-40	55-70, 30-60, 65-30	50-45 50-35
4	120-110, 110-90, 105-100	100-140 100-100	105-100, 95-125, 125-115	90-115 180-95	100-115, 100-120, 145-95	110-60 95-115
5	80-40, 45-65, 35-65	45-60 10-120	40-65, 55-60, 25-80	55-80 45-80	70-60, 45-90, 40-80	45-70 60-55
6	60-55, 35-65, 60-60	40-95 50-55	70-55, 60-50, 90-45	35-75 55-55	35-80, 70-45, 85-50	80-55 60-45

*Pairs of trials, first trial ascending in delay time, second trial descending in delay time.

Table A10. Temporal Bands
Subject R.S.

Preliminary Trials Delays, msec

Dark to Bright	20	0	20	0	15	10	-15	-20	10	0
Bright to Dark	30	30	30	-30	-30	10	25	15	-10	0

Length of the Temporal Bands, msec

Measuring Point	Slope, msec 600		450		300	
1	155-90,* 160-145, 150-165	95-160 170-140	155-140, 130-170, 160-165	160-145 140-145	160-150, 140-155, 150-155	170-120 160-140
2	125-140, 150-105, 165-55	110-140 145-140	165-90, 200-105, 100-160	90-165 85-115	155-115, 170-90, 130-135	175-35 150-100
3	135-65, 70-125 115-95	85-105 115-130	140-75, 85-100, 105-90	55-165 105-75	30-95, 115-70, 70-155	75-85 85-100
4	205-180, 195-190, 205-200	180-180 220-145	185-175, 190-205, 150-200	175-205 170-185	200-180, 175-190, 175-210	200-185 210-195
5	160-150, 170-140, 145-145	160-140 140-145	175-150, 155-140, 150-135	165-150 140-155	140-155, 125-160, 145-155	150-155 165-200
6	155-80, 30-255, 40-105	90-200 225-140	60-85, 105-135, 85-150	85-165 -5-200	65-180, 160-150, 185-155	170-140 125-160

*Pairs of trials, first trial ascending in delay time, second trial descending in delay time.

The vita has been removed from the scanned document

TEMPORAL ENCODING IN THE VISUAL SYSTEM

by

Maier Almagor

(ABSTRACT)

A new model for temporal and spatial encoding in the visual system is developed and presented. The model indicates that spatial information is encoded in a manner similar to the encoding of temporal information. Experimental evidence related to this model is presented and analyzed.

The temporal part of the model has been further developed. The model is based on two integrators in series with a temporal differentiator. The outputs of a varying number of similar, surrounding parallel cells can be pooled together in spatial integration.

The length of the integration time as well as the number of cells spatially pooled together are controlled by the amount of spatial and temporal integrated light falling in and around every point on the retina.

Three series of experiments were conducted to validate the model. The experiments used (1) a TV display of random, dynamic noise and (2) a specially developed stimulus generator which is able to produce very large homogeneous visual fields which can be easily modulated to reproduce a large variety of temporal waveforms having a rise time

longer than 1 msec.

The obtained results support the proposed model. The principal findings are: (1) Time integration of the eye is locally controlled and set across the retina and has very fast dynamics. (2) The obtained CFF curves suggest a correlation between the frequency at which maximum sensitivity is obtained and the sensitivity itself. (3) As predicted by the model, temporal bands are developed in the visual system for stimuli showing temporal discontinuity points. The width of the temporal bands was measured and a strong correlation was found between the temporal band width and the integration time. The width of the temporal bands is a function of the luminance level at which they are produced; it is not dependent on the stimulus slope. The apparent brightness of the temporal band is, however, dependent on the slope of the stimulus.

The present findings about the temporal and spatial integration of the eye-brain system suggest that they work as a fast adaptation mechanism and that they play a central role in visual perception, explaining homogeneously such disparate phenomena as the spatial Mach bands and their assymetry, the Broca-Sulzer effect, and backward masking.

Suggestions about further research are offered.